European Commission

JRC TECHNICAL REPORTS

Black Sea ecosystem model: setup and validation

Svetla Miladinova
Adolf Stips
Elisa Garcia-Gorriz
Diego Macias Moy

2016

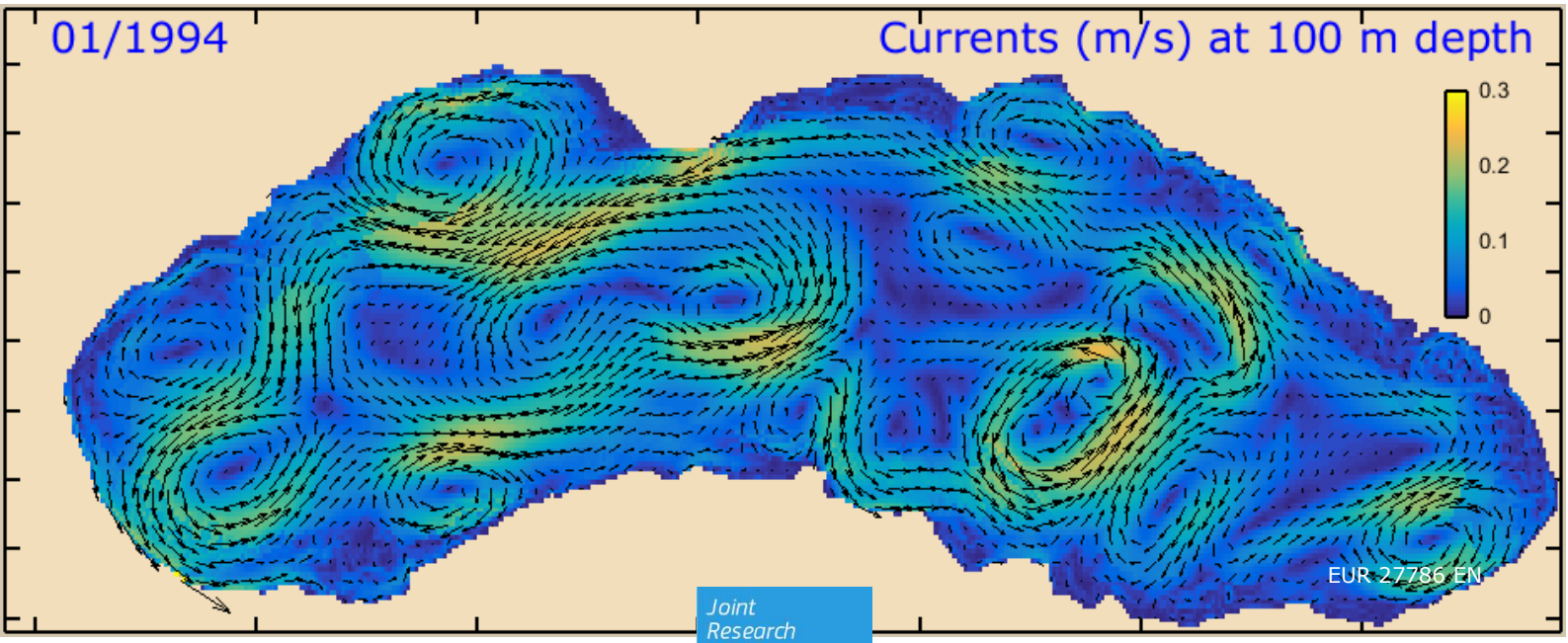

Joint Research Centre

Black Sea ecosystem model: setup and validation

This publication is a Technical report by the Joint Research Centre, the European Commission's in-house science service. It aims to provide evidence-based scientific support to the European policy-making process. The scientific output expressed does not imply a policy position of the European Commission. Neither the European Commission nor any person acting on behalf of the Commission is responsible for the use which might be made of this publication.

Contact information
Name: S. Miladinova-Marinova
Address: Joint Research Centre, Via E. Fermi, 2749 – TP27, 21021 Ispra (VA), Italy
E-mail: svetla.miladinova@jrc.ec.europa.eu
Tel.: +39 0332 785347

JRC Science Hub
https://ec.europa.eu/jrc

JRC100554

EUR 27786 EN

ISBN 978-92-79-57237-1

ISSN 1831-9424

doi:10.2788/601495

How to cite: Svetla Miladinova, Adolf Stips, Elisa Garcia-Gorriz, Diego Macias MoyAuthors; Black Sea ecosystem model: setup and validation; EUR 27786; doi: 10.2788/601495

Table of contents

Acknowledgements

This work was supported by EU-MC 33764 SIMSEA project.

Abstract

In the framework of EU-MC project SIMSEA, a modelling study has been initiated to validate the General Estuarine Transport Model (GETM) for Black Sea's simulations. The model is forced with atmospheric data from the European Regional Downscaling Experiment (EURO-CORDEX), river runoff from Global Runoff Data Centre (GRDC) and is initialised with temperature and salinity 3D fields coming from the project MEDAR/MEDATLAS II. Simulations are performed in a closed basin configuration with boundary conditions at the Bosphorus strait ensuring a net zero water flux balance in the Black Sea. An accurate method to calculate the optical depth estimated from satellite data has been involved. The model has been validated against measured/calculated temperature and salinity fields. The simulations with our hydrodynamic model correctly capture the Black Sea's hydrodynamics – the strong halocline at 70-150 m, the Cold Intermediate Layer (CIL) at ~70 m, the doming of the isohalines due to the cyclonic Rim current, sea surface temperature variation, etc. A new Black Sea Ecosystem Model (BSSM) is linked via the Framework for Aquatic Biogeochemical Models (FABM,) with our hydrodynamic model. The coupled physical-ecosystem modelling system has been also calibrated and validated for the Black Sea runs. The numerical experiments indicate that the biogeochemical components of the model rather successfully reproduce the main features and state variable evolution in the Black Sea ecosystem: the growth in phytoplankton biomass and changes in seasonal cycles of the main ecosystem components. It is concluded that the physical processes are important for a reliable reproduction of seasonal and inter-annual changes in the ecosystem.

1. Introduction

A vision for clean, healthy, safe, productive and biologically diverse oceans and seas is the basis for managing sustainable human use and exploitation of the goods and services provided by the seas. Numerical modelling supports the development of methods to describe the state of the ecosystem and mechanisms to minimize the impacts of human activities to avoid undesirable disturbances. The marine models developed within the Water Resources unit highlight regions at high risk of physical and biochemical change, such as oxygen depletion events and eutrophication. Development of a marine knowledge base that focuses on physically and biologically sensitive areas is necessary to support marine spatial planning measures that integrate ecosystem and biodiversity conservation. Marine modelling at JRC provides a tool to examine the marine ecosystem and results from the various setups can inform and support a variety of EU policies including the Marine Strategy Framework Directive (MFSD). Because in Europe the implementation process of the MFSD in the Black Sea region is the least developed we focus for this project on the marine ecosystem of the Black Sea.

This is further relevant as the Black Sea has suffered from severe ecological changes since the 1970s due to concurrent effects of intense eutrophication associated with excessive anthropogenic nutrient load and pollutants, trophic cascades as a result of overfishing and outburst of gelatinous carnivores as well as natural climatic variations.

The main objective of the SIMSEA project is to implement an advanced ecosystem model for the complex Black Sea ecosystem based on the validated JRC hydrodynamic model to generate future scenario simulations considering different policy options and climate change scenarios. To achieve this ambitious goal, the project has been split into three sub-objectives: first to define model parameters for key processes, testing and model validation as well as assessing and developing the scenarios, second to run the scenarios by changing climate and anthropogenic drivers and determining their impacts on the ecosystem and third to disseminate the gained knowledge, expertise and skills from the project to a broad audience with an interest in its results and publish in peer-reviewed journals.

Following the SIMSEA work plan this first report focuses on the first activity, namely model setup, calibration, (definition of model parameters), sensitivity testing and validation.

2. Hydrodynamic model setup and validation

2.1 Study area

The Bosphorus Strait connects the Black Sea with the Mediterranean Sea via the Marmara Sea and the Kerch Strait is the connection with the Azov Sea (Fig.1). The shelf edge slope is steep and the shelf is basically narrow except for the north-western shelf region. In this region several big rivers discharge, namely, the Danube, Dniepr and Dniestr. In addition to these rivers, the Rioni, Sakarya, Kizil Irmak, Coruhsuyu, Yesilirmak and many other small ones discharge into the Black Sea. Buoyancy due to river runoff is an essential reason for the basin wide cyclonic circulation the so called Rim Current with well exhibited western and eastern gyres (Oguz, 1995). The general circulation of the Black Sea is driven by this large freshwater input on the north-western shelf as well as wind stress and is determined by the steep topography around its periphery that consists of narrow shelves and a maximum depth of around 2200 m (Oguz et al., 2004). The eddy dominated circulation exhibits different types of structural organizations within the interior cyclonic cell, the Rim Current flowing and meandering along the sharply varying topography. The interior circulation comprises several sub-basin scale gyres, each of them involving a series of cyclonic eddies that interact among each other. The presence of a series of recurrent, near-shore, anti-cyclonic eddies between the Rim Current and the coast, along with a number of cyclonic gyres in the

basin's central area, have been confirmed by both satellite data and by hydrographic observations (see the review in Oguz et al., 2004).

Positions where profiles from 3D model simulations have been analysed (see Fig.1) are chosen in order to present Black Sea's dynamics at: b1 and b2 - centres of the main cyclonic gyres, b3 and b4 - from the basin interior but close to Rim Current and anti-cyclonic eddy, b5 in the central area occupied by western or eastern gyre, b6 and b7 – locations where in situ data predominantly exist, and b8 and b9 – from the north western and north eastern shelf.

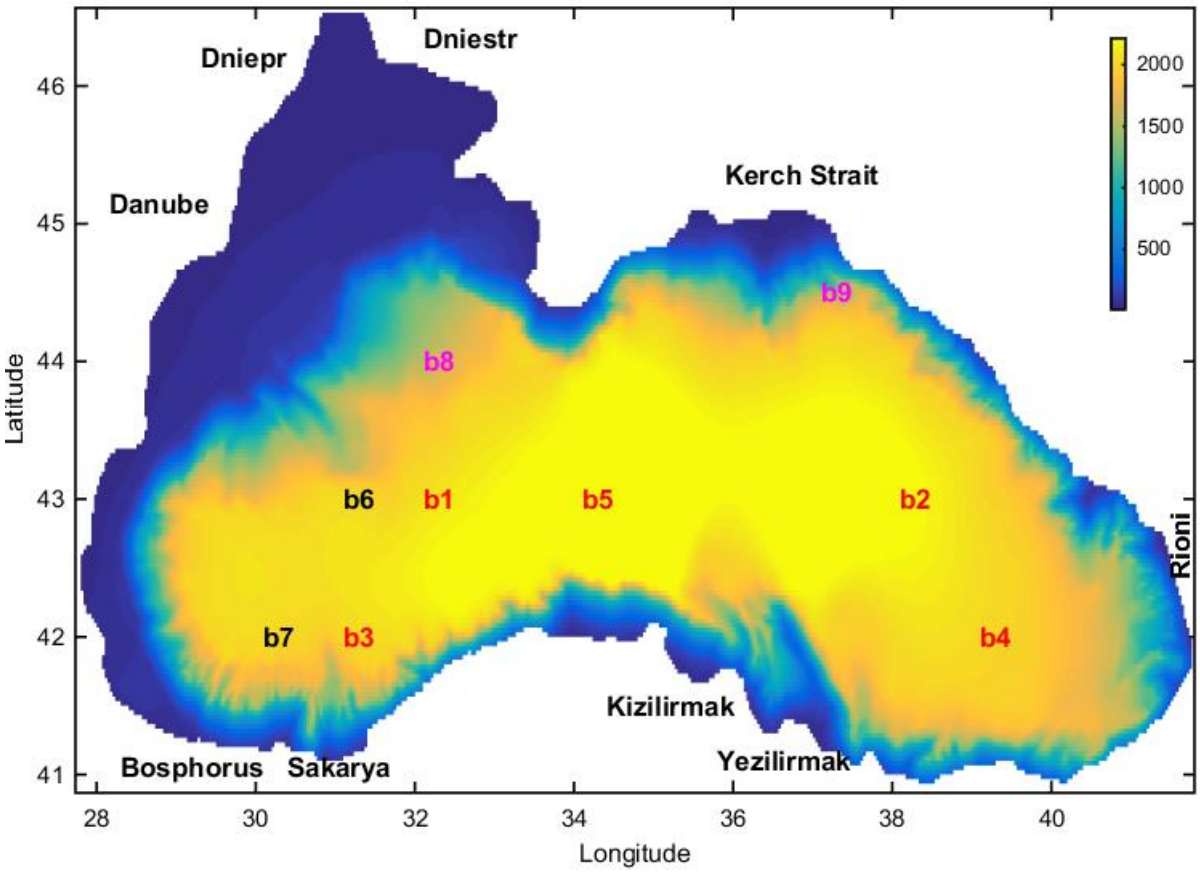

Figure 1. Geographic location, model bathymetry and major rivers of the Black Sea. The positions where profiles from model simulations and other model data have been analysed are numbered in the order that they met in the text: b1 - 43°N and 32°E, b2 - 43°N and 38°E, b3 - 42°N and 31°E, b4 - 42°N and 39°E, b5 - 43°N and 34°E, b6 - 43°N and 31°E, b7 - 42°N and 30°E, b8 - 44°N and 32°E, b9 – 44.5°N and 37°E.

Simulations for model sensitivity analysis and validation start in 1990 and they are run for at least five years. The choice of the starting year is done on the base of available data for temperature and salinity initialisation. Preliminary tests have indicated that hydrodynamic model is insensitive to the month in which the concrete run begins. The period of testing runs is in the last decade of twentieth century because of existing model/reanalysis and measured data (Beşiktepe, 2003; Zatsepin et al., 2003)

2.2 Model initialisation and forcing

2.2.1 River runoff

Only major rivers discharging into the Black Sea are used in the model simulations. Every river varies seasonally and adds a fresh water volume to the model grid box,

which is nearest to the geographical position of its mouth. Thus it affects the sea level and currents, but also the salinity in this grid box, which is calculated as a mean from the salinity of the previous time step and the total added volume. The climatological values from the Global Runoff Data Centre (GRDC, http://www.bafg.de/GRDC) for these rivers are shown in Fig.2, in descending order of importance. The inflow of low salinity water (11 ‰) from the Kerch Strait is considered in the model like river runoff. According to the GRDC data set the Danube River has a mean annual discharge of 6365 (m^3s^{-1}), Dniepr - 1631.8 (m^3s^{-1}), Rioni - 409.7 (m^3s^{-1}), Dniestr - 326.3 (m^3s^{-1}), Sakarya – 217.3 (m^3s^{-1}), Coruhsuyu - 197.7 (m^3s^{-1}), Kerch Strait- 185.6 (m^3s^{-1}), Yesilirmak - 185.4 (m^3s^{-1}) and Kizilirmak - 180.5 (m^3s^{-1}). In percentages the Danube River accounts for about 65.6% of the total runoff and Dniepr for16.8%. In Fig. 3 and 4 data extracted from four different climatological data sets is compared for the Danube and Dniepr. The data sets are GRDC, Global River Discharge Database (RivDIS) (http://www.daac.ornl.gov), University Corporation for Atmospheric Research (UCAR) (http://rda.ucar.edu/datasets/ds552.1/) and Naval Research Laboratory (NRL).

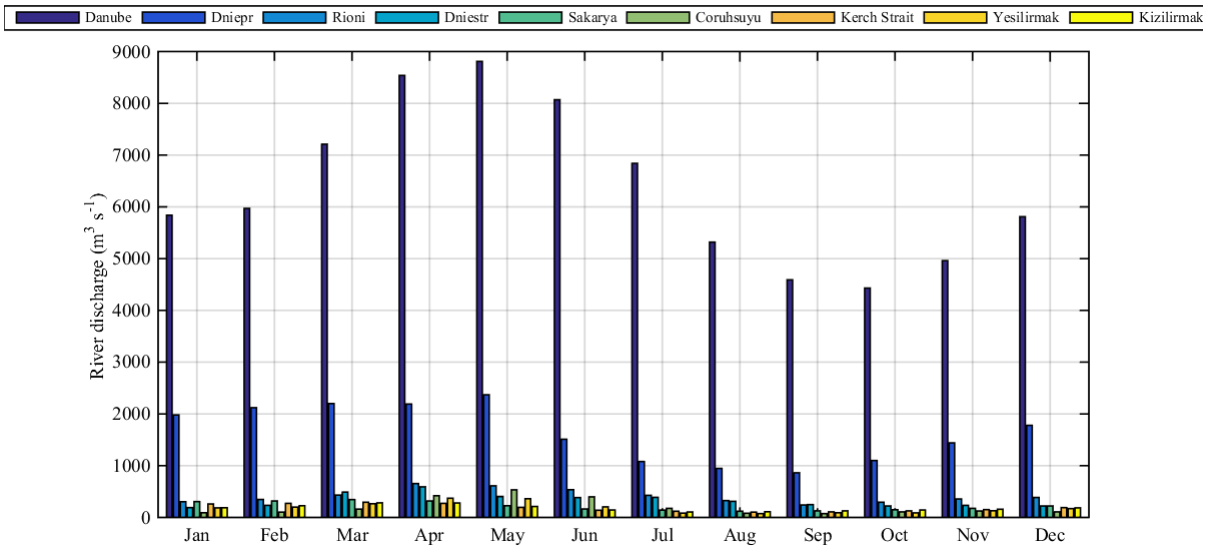

Figure 2. Climatological monthly mean discharge values for the rivers under consideration and Kerch Strait according to GRDC data set.

Table 1. Mean annual river discharge of GRDC and RivDIS and their statistical comparisons.

River	Mean annual discharge (GRDC) (m^3s^{-1})	Mean annual discharge (RivDIS) (m^3s^{-1})	Absolute mean error %	Correlation coefficient	Root mean square difference (m^3s^{-1})
Danube	6365.83	6498.56	-2.08	0.9982	160.68
Dniepr	1631.58	1483.43	9.08	0.8207	376.89
Rioni	409.67	408.5	0.28	1.0000	1.256
Dniestr	326.33	375.04	-14.93	0.9785	56.50
Sakarya	217.42	192.85	11.3	0.9609	34.60

Kizilirmak	180.5	202.18	-12.01	0.9970	23.45

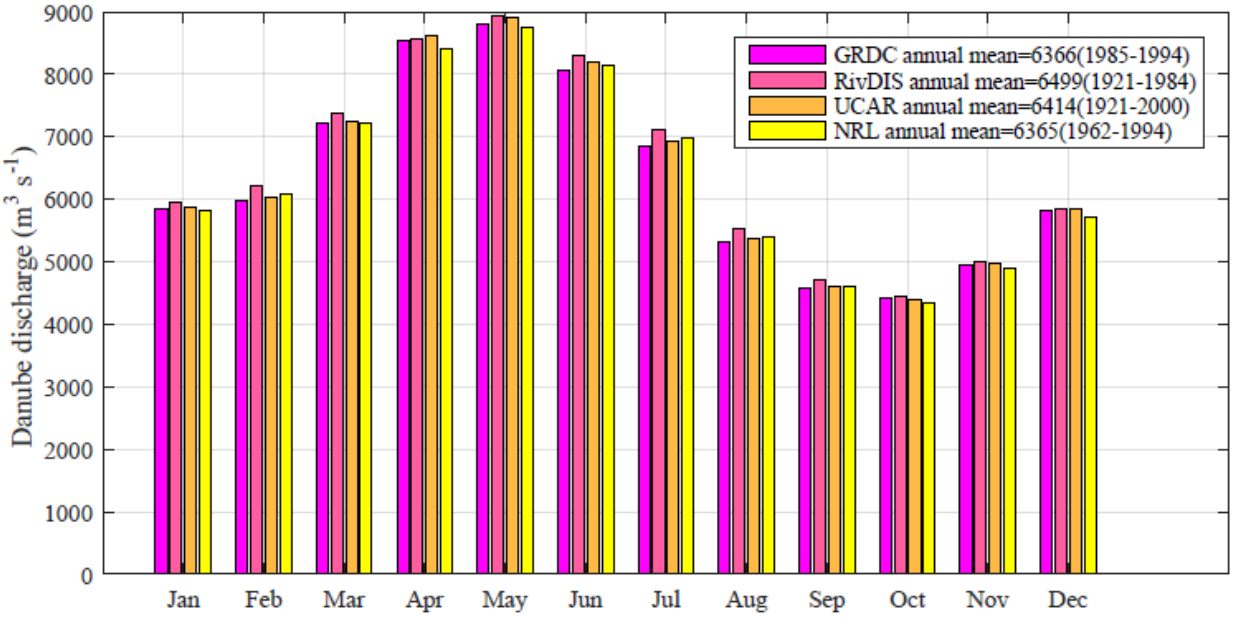

Fig.3. Climatological mean annual cycle of the Danube River from four different climatological data sets.

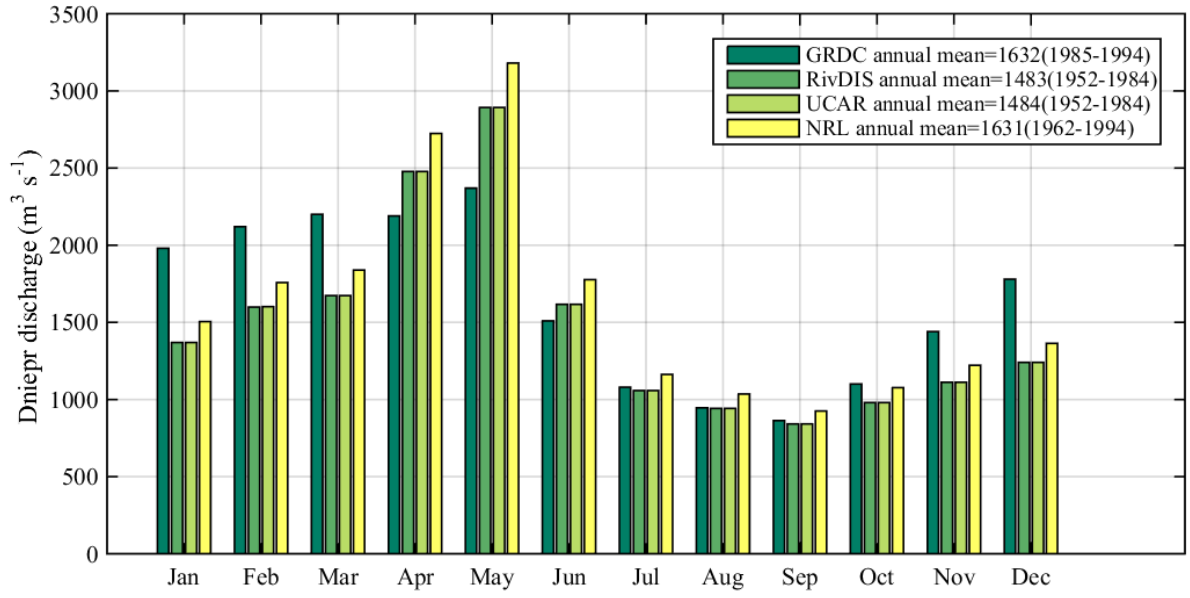

Fig. 4. Climatological mean annual cycle of the Dniepr River from four different climatological data sets.

Figure 3 indicates that all presented data sets generally agree closely for the Danube discharge. On the contrary in Fig. 4 is evident a deviation for the Dniepr river. There is a need for statistical analysis to clearly examine differences in monthly/annually mean discharges. In Table 1 are presented the annual mean discharges of GRDC and RivDIS for six big rivers and statistical comparisons between them. Absolute mean error is calculated as a difference between GRDC and RivDIS annual mean values divided by

annual value of GRDC. Negative values indicate that RivDIS annual values are larger than GRDC ones. Basically, annual values differ by more than 9% for four of the rivers. Almost all of the variance in the RivDIS discharges is similar to that of GRDC discharges because the correlation coefficient is > 0.9. Correlation values and the root mean square difference values support the conclusions that we have already came across from bar plots in Figs. 3 and 4, namely that climatological values of the four datasets are close to each other except for the Dniepr River. Runoff forcing in the current model is done by GRDC since it contains not only climatological data but also monthly mean discharge data for the Danube River.

2.2.2 Meteorological forcing

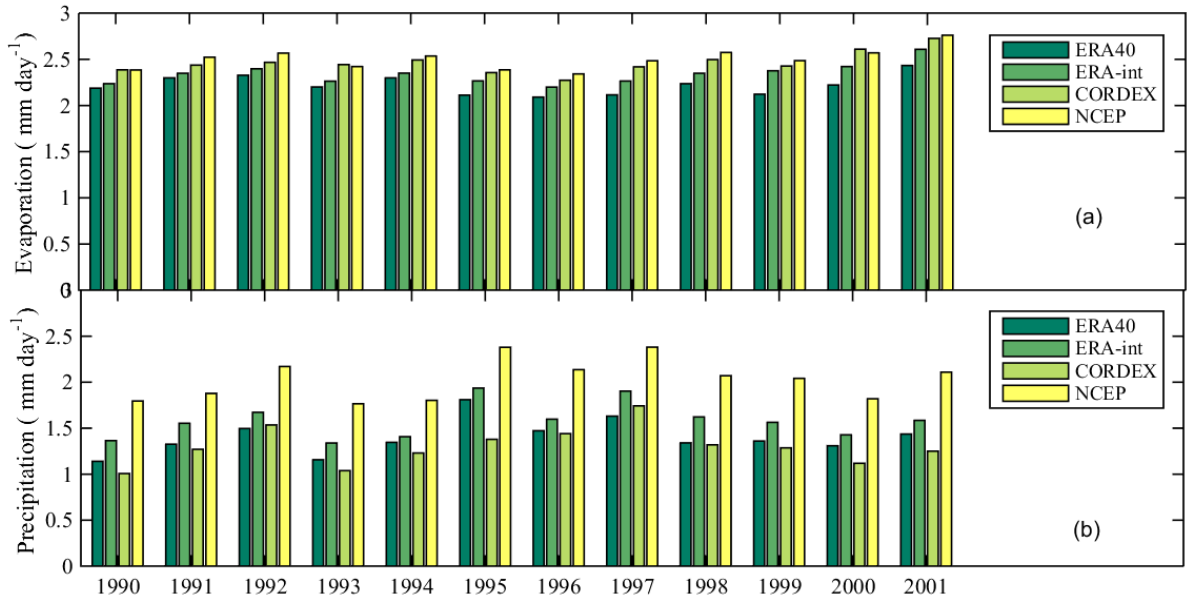

Figure 5. Annual mean values of (a) evaporation and (b) precipitation over the Black Sea calculated using different climate forcing.

Basically, the Black Sea has a positive freshwater flux due to excess of precipitation and river runoff over evaporation. Figure 5 illustrates annual mean values of evaporation/precipitation from 1990 to 2001 extracted from four different historical climatological reanalysis data, namely, ERA-40 (apps.ecmwf.int) (1980-2001); ERA-int (www.ecmwf.int) (1980-2010); downscaled CORDEX erain forcing based on the International Panel for Climate Change (IPCC) Climate Model Intercomparison Project (CMIP5) scenarios for Europe (www.cordex.org) (1989-2008); NCEP (National Centers for Environmental Prediction (http://www.esrl.noaa.gov) (1989-2002). GETM is reading the precipitation data from the meteorological file, but calculating evaporation and condensation inside of GETM. This method has the advantage that the calculated humidity flux is consistent with the calculated latent heat flux. ERA40 and NCEP appear to result in the lowest and highest evaporation values, respectively. Evaporation (Fig. 5 a) does not vary considerably between both years and datasets, having a minimum value 2 mm day^{-1} and a maximum value 2.9 mm day^{-1} during period considered. Contrary, precipitation varies a lot – from 1 mm day^{-1} to 2.3 mm day^{-1} and differences over datasets are significant. For example, in 1990 the four datasets provide 1.14, 1.37, 1.01 and 1.04 mm day^{-1} in the order that they are listed in Fig. 5. On the base of these datasets the seasonal cycle of evaporation/precipitation is also calculated (Fig. 6). All reanalysis estimates show a similar seasonal cycle for evaporation (Fig. 6 a), with

minimum values in April and maximum values in August. Evaporation over the Black Sea is mainly wind driven and is largest over the western side where the winds are stronger (Romanou et al., 2010). Once more, reanalysis data give distinct seasonal values for precipitation (Fig. 6 b), with higher precipitation in winter and lower in late spring and summer. The largest is the difference between CORDEX, which estimates the highest precipitation values, and NCEP, which gives the smallest ones in the second half of the year. The NCEP data product stands out from the other three datasets both in terms of the mean annual and seasonal precipitation over the Black Sea. CORDEX and ERA-int atmospheric reanalysis are preferred to be used in model sensitivity analysis.

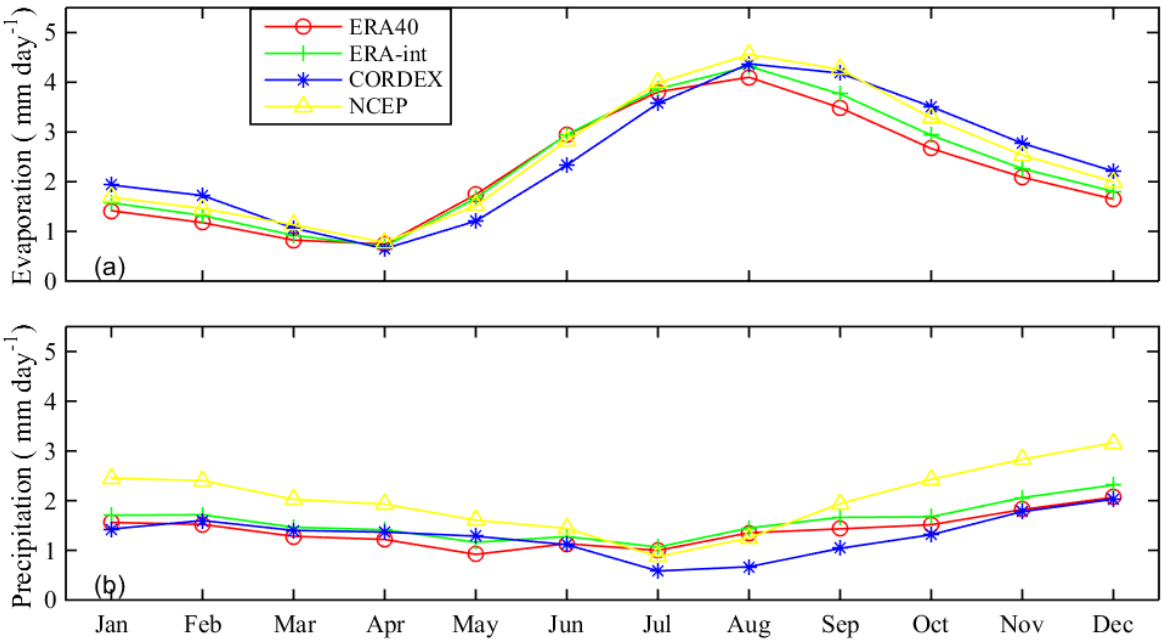

Figure 6. Calculated mean annual cycle of (a) evaporation and (b) precipitation according to ERA-40, ERA-int, CORDEX and NCEP datasets.

2.2.3 Freshwater budget and Bosphorus fluxes

The freshwater input, which is the sum of river runoff and precipitation minus evaporation, displays a seasonal cycle (Fig. 7 a) with maximum values in spring and minimum ones in summer. Because of high evaporation/precipitation differences (Fig. 6), the differences in freshwater budget are evident, particularly the differences between CORDEX and NCEP data. For example ERA40 gives lower values than ERA-interim for both evaporation and precipitation, and finally the resulting freshwater flux is similar. Let's explore the ranges of forcing variability responsible for the water flux changes.

The constant increase of the sea level caused by the freshwater surplus is counteracted/balanced by the corresponding outflow through the Bosporus. The transport through the Bosphorus is vertically separated in two parts: bottom inflow and surface outflow. Based on long-term averages of the salinity along the northern end of the strait, and assuming steady-state mass budgets, Ünlüata et al., (1990) evaluated mean annual volume transports in the upper and lower layers to be about 19406 m^3 s^{-1} and 9893 m^3 s^{-1}. These values were later updated, for example, by Beşiktepe et al., (1994) and Tuğrul et al., (2002). An estimate of volume fluxes calculated by a quasi-stationary hydraulic two-layer model of the strait with bottom and interface friction is given in Maderich and Konstantinov (2002). In general, the largest fluxes in both layers are usually observed in spring, whereas the lowest volume transports in the strait are usually recorded in fall (Tuğrul et al., 2002). Because our simulations are performed in a

closed basin configuration, the excess of freshwater and Bosphorus inflow should be balanced by the Bosphorus outflow. However, the freshwater input (Fig. 7 a) depends on the choice of climate and runoff forcing and varies both seasonally and between the years (Fig. 5). An important factor for the freshwater input is the net difference between precipitation and evaporation. For example, annual values of precipitation and evaporation, which are shown in Fig. 5 in the period from 1990 to 2001, demonstrate that the Bosphorus exchange has to be annually resolved and adjusted in accordance with the climate forcing applied.

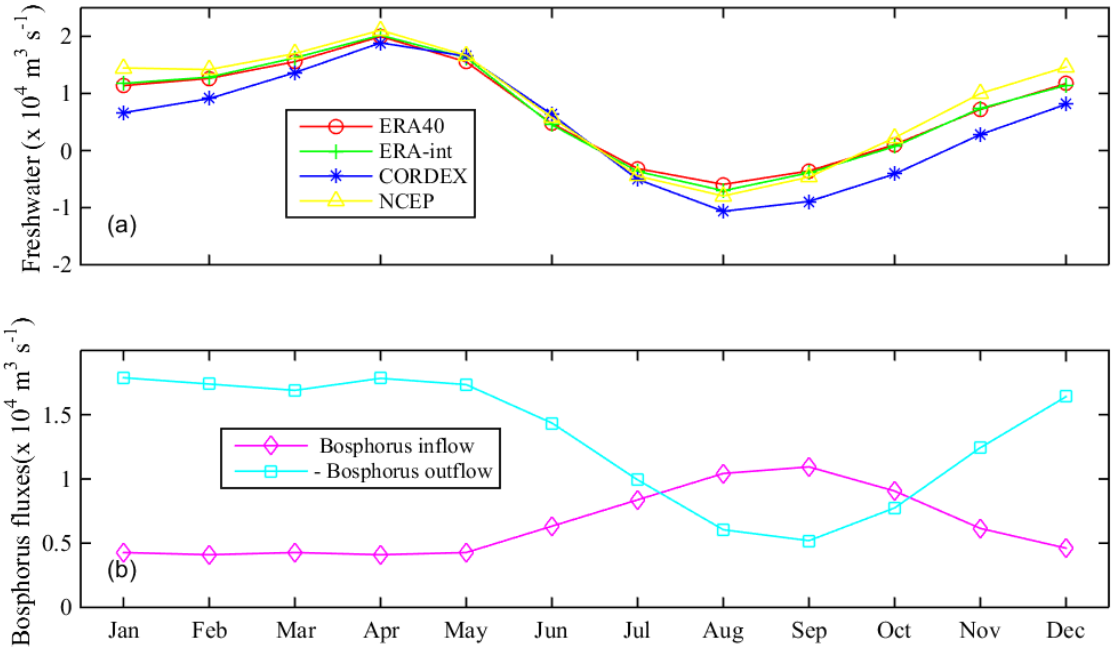

Figure 7. (a) Freshwater input to the Black Sea calculated on the base of GRDC runoff forcing and four different atmospheric forcing. (b) Climatological Bosphorus fluxes: Bosphorus inflow – lower layer; Bosphorus outflow – upper layer as reported in Maderich and Konstantinov (2002).

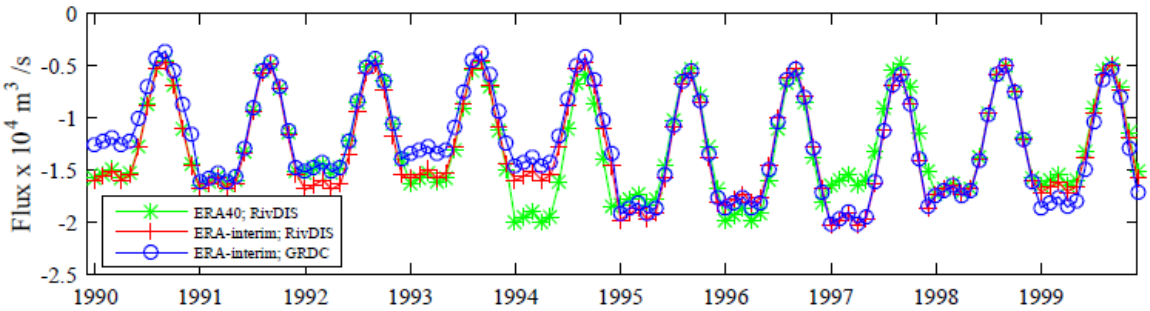

Figure 8. Adjusted outflow from the Bosphorus strait x 10^4 m^3 s^{-1} in accordance with: ERA40 and RivDIS (green); ERA-int and RivDIS (red); ERA-int and GRDC (blue).

In Maderich and Konstantinov (2002) the outflow and inflow in the Bosphorus straits can be estimated by the functions depicted in Fig. 6 b with annual mean values of 13089 m3/s and 6459 m3/s in the upper and lower layer, respectively. These functions are used here as initial values for the Bosphorus outflow/inflow. Then, the values are updated annually in order to keep the sum of inflow and outflow equal to freshwater input. An illustration of the corrected Bosphorus outflow is given in Fig. 8 for the case of

RivDIS and GRDC runoff and ERA40 and ERA-int climate forcing for a 10 year period. The three time series given in Fig. 8 differ significantly in certain years and overlap in others. However, in all cases corrections are required as it is evident from the time series of the annual basin elevation (m) using ERA-interim and GRDC datasets together with climatological inflow/outflow from Fig. 7 b. Mean annual elevation in the case without adjustment of the Bosphorus volume flux, which is denoted with cyan diamonds in Fig. 9, exhibits strong alterations leading to artificial near sea surface mixing. The other three time series presented in Fig. 9 show small annual basin elevation when the Bosphorus outflow is corrected (as depicted in Fig. 8). Although with both ERA40 and ERA-interim we tried to approximate zero net flux, there is a small but consistent increase in sea level. The deviation could come from error accumulation when averaging basin wide evaporation/precipitation values. Therefore the corrected profiles in Fig. 8 are further multiplied by 1.02 and the resulting annual elevation is given in Fig. 9 (green, red and blue symbols). The lower Bosphorus layer is treated as an inflowing river, with a salinity of 36 - 38, while the upper outflow has the salinity of the grid box.

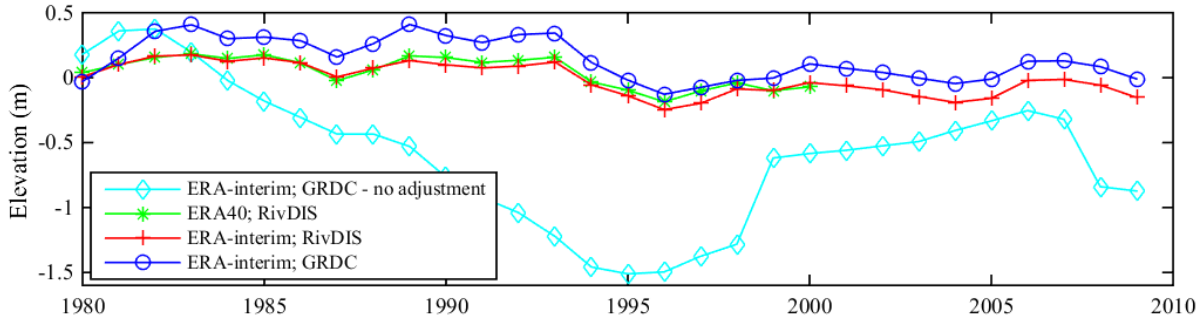

Figure 9. Annual mean elevation of the Black Sea in m, calculated for different forcing setups.

2.2.4 Temperature and salinity initialisation

The model is initialised with temperature and salinity 3D fields coming from the project MEDAR/MEDATLAS II (http://www.ifremer.fr/medar). The MEDAR data set for the Black Sea reflects the main features known from observations – the strong halocline at 70-150 m, the Cold Intermediate Layer (CIL) at ~70 m and the doming of the isohalines due to the cyclonic Rim current. In Fig. 10 are presented MEDAR climatological contours at b1 and b2 (see Fig. 1). Climatological mean values of MEDAR are calculated on the base of data from the last decade of twenties' century so we decided to start our calculations in 1990.

The Cold intermediate layer, which is characterised by temperatures less than 8°C, is a special feature of the Black Sea. This low temperature layer is usually located below the seasonal thermocline and can be seen throughout the deep basin. The CIL is preserved throughout the year by strong vertical gradients in the permanent pycnocline that prevent the water in the CIL from mixing with adjacent layers. It is formed by convective processes associated with the winter cooling of surface waters (Ovchinnikov and Popov (1987), Oguz et al., 1991) and cool fresh water from north-western region. For both mechanisms of formation the severity of winter conditions determine the volume of CIL formed. Formation is limited to the upper layer because vertical advection is stopped at the halocline by the strong stratification (the Brunt-Vaisala frequency, N^2, ranges from 50 to > 200 hr^{-2} in the upper 200 m (see Murray et al., 1991). The large river input results in strong vertical stratification with a fresh, lower density layer at the surface and a salty higher density layer in the deep water (even though the deep water of the Black Sea is much less saline than typical ocean seawater), as shown below. It is important to note that the only source of salt water is through the Bosphorus. The Bosphorus inflow

can sink to the bottom or may go to an intermediate depth and spreads horizontally on the isopycnal surface appropriate to its density.

The temperature varies seasonally in the near surface layer due to solar heating and decreases with depth to a minimum located at a depth of approximately 50 m in the central basin and as deep as 100 m near the margins (Oguz et al., 1991). Then it increases to a value of about 8.75°C at 200 m and does not vary considerably deeper into the sea where it reaches a maximum value of about 9°C. Obviously, the vertical variation of temperature is very different from that in the global ocean.

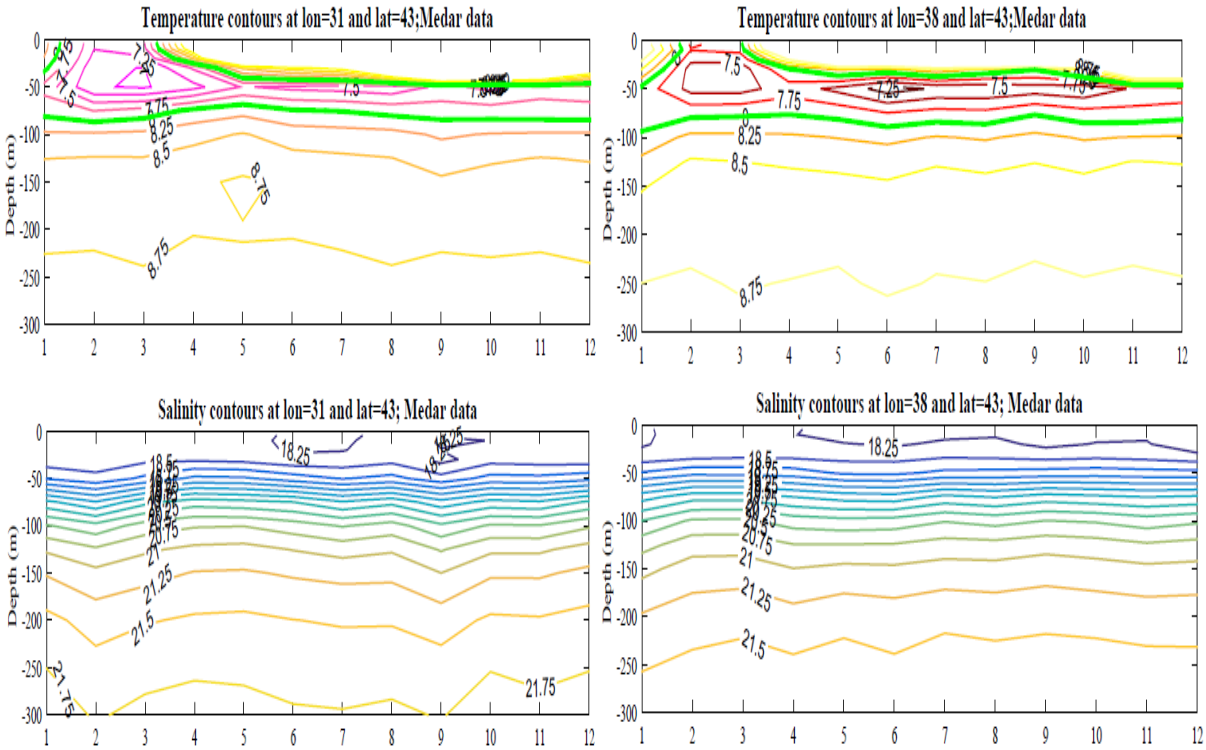

Figure 10. Annual cycle of MEDAR climatological temperature and salinity contours from the surface to 300 m depth at b1 (left pannel), and b2 (right pannel).

2.2.5 Spatial grid and bathymetry

The choice of the proper vertical resolution is of crucial importance for the Black Sea. The presence of the Cold Intermediate Layer requires a sufficient number of vertical layers to adequately represent the processes between the constant halocline and seasonal thermocline. Exploiting the GETM feature of providing general vertical co-ordinates we tested different layer distributions, with the layer number from 35 to 70 layers. From this sensitivity study we obtained best results when using 50 layers and a uniform distribution of layers down to 50 m.

The bathymetry data source used in this study is ETOPO1 global bathymetric grid with horizontal resolution of 1 min (https://www.ngdc.noaa.gov/mgg/global/). Linear programming procedure was applied to smooth the ETOPO1 bathymetry. Then two data sets were created with different horizontal resolution –2 min (topo2) and 3 min (topo3). Results given in Fig. 11 were achieved by the use of topo3 grid. CIL upper and lower boundaries are defined by the 8°C isotherm. However, the CIL usually disappears in the eastern part of the sea. At the same time, simulations, which were performed with topo2 better represented the Black Sea dynamics. For comparison, mean temperature/salinity contours calculated using topo2 grid in the same location b2 are plotted in Fig. 12. The

CIL is maintained during the whole period of simulations (from 1989 to 1999). Cold water current from the north-western that replenish farther the CIL in the east part of the open sea was better represented by using topo2. The depth of the CIL is not precisely represented in Fig. 12 because of the constant attenuation coefficient applied (see next the paragraph). Both runs are forced with ERA-int meteorological forcing. Finally, we decided to continue with the 2 min grid, which guarantees that the CIL will be maintained (see Figs. 14-15) at a reasonable computational effort.

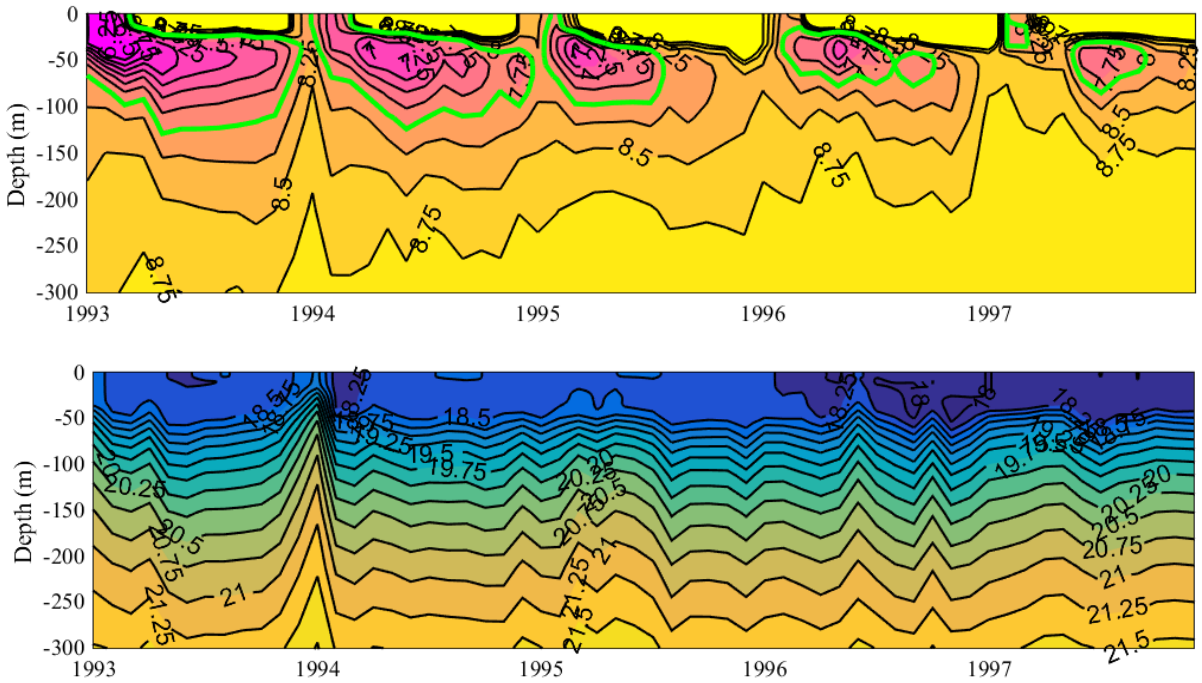

Figure 11. Monthly mean contours of temperature (°C) (upper panel) and salinity (lower panel) from the surface to 300 m depth calculated on topo3 at b2.

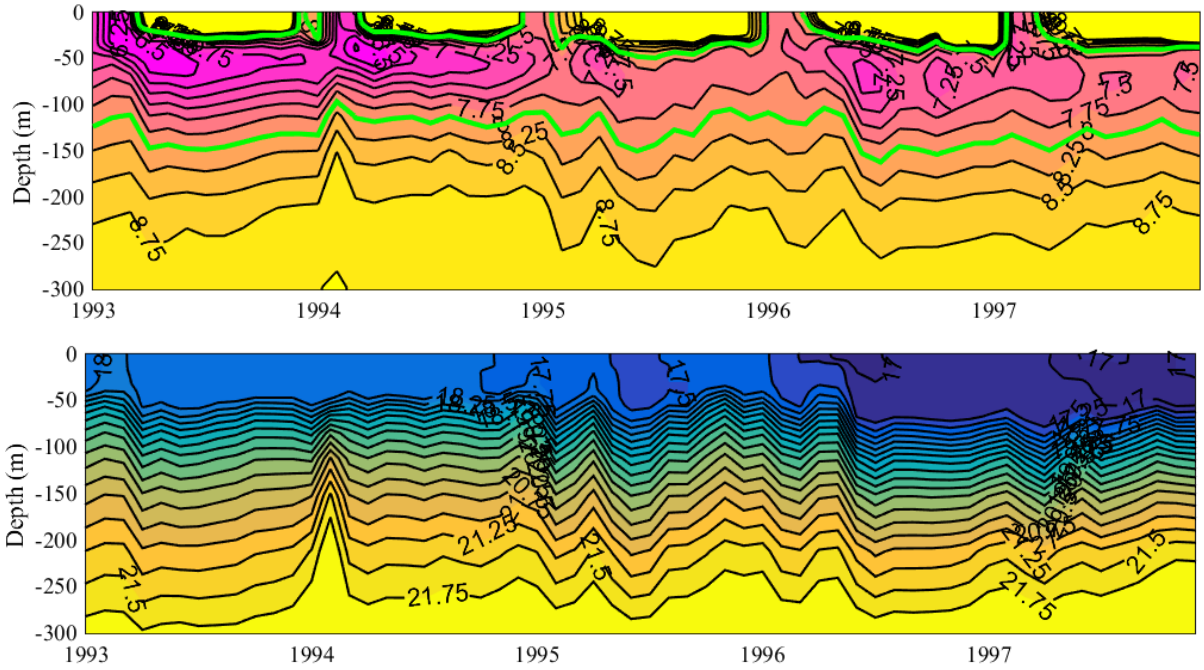

Figure 12. The same contours as in Fig. 11, however, calculations were done on topo2.

2.2.6 Short-wave radiation – underwater attenuation method

The two-component wavelength (red and blue light) exponential decay model of Jerlov's type model was used to calculate penetrating shortwave radiation fraction: $(1-A)\exp(-z/\gamma_1)+\mathrm{A}\exp(-z/\gamma_2)$, where γ_1 and γ_2 are attenuation lengths of red (near surface) and blue (deep) light, respectively; A is attenuation coefficient and z is the distance from the surface. The applied attenuation coefficients are the same everywhere in time and space. This however, resulted in insufficient simulation of the CIL dynamics (Fig. 12). A more accurate method for evaluation of water optical characteristics using optical depth estimates from satellite data has been developed. Here we have used fixed values for A and γ_1, while γ_2 varies spatially and temporally. The SeaWiFS (http://oceancolor.gsfc.nasa.gov/SeaWiFS) ocean colour data base is used to estimate the water optical depth on monthly bases.

2.2.7 Long-wave radiation

The longwave radiation is the difference between the energy radiated from the sea surface ($\sim T^4, T$ ocean skin temperature) and that received from the sea by the atmosphere (heat loss to ocean), mostly determined by water vapour in lower atmosphere $\sim T^4, T$ atmospheric temperature). It does not change much seasonally, or with location. Effect of cloud is significant. The longwave radiation is typically the largest contribution to the all heat fluxes. Incoming global mean is ~400 W m^{-2}, outgoing 330 W m^{-2}. The net flux is the difference between two rather crude approximated contributions and there is the largest source of uncertainty for our heat flux.

Net long wave radiation according to the Josey et al., 2003 formula, considering the effect of water vapour is in the moment the best available parameterization in GETM.

2.3 Hydrodynamic model simulations

2.3.1 Sensitivity analysis

In paragraph 2.2.3 was explained that the model is highly sensitive to river runoff and atmospheric forcing, such as both play an important role in the estimation of water/salt fluxes through the Bosphorus Strait. Here the sensitivity of sea surface temperature (SST) to atmospheric forcing and underwater attenuation method is done.

Several error measures (bias, root mean squared error (RMSE), correlation and histograms) are used to assess the differences between simulated herein SST and satellite data. Results of 4 separate model runs forced with CORDEX or ERA-int and with two different values of A are shown in Fig. 13. The diagram shows the model to reference statistics for the annual (blue), Jan-Mar (red), Apr-Jun (green), Jul-Sep (yellow) and Oct-Dec (magenta) SST during the period 1990-1996. Model SST is calculated as average temperature in the upper 2.5 m of the Black Sea's surface water. Reference values in Fig. 13 are taken from the Pathfinder climatology (available at http://data.nodc.noaa.gov/pathfinder/CoralAtlas/PathfinderSST_Climatologies/). The coefficient A investigated here has a typical range from 0.54 to 0.79 (Kara et al., 2005). Generally, the best model performance is achieved for winter months with both CORDEX and ERA-int forcing for $A = 0.65$, while the highest misfit is found for the summer/fall months and CORDEX forcing. Annual SST values from all four runs have standard deviation of the same order as the Pathfinder's SST and correlation between model SST and satellite data is in the range from 0.9 to 0.94. Alteration of coefficient A influences predominately calculated SST in summer/fall months. It appears, that runs with ERA-int forcing are less sensitive to the attenuation constant.

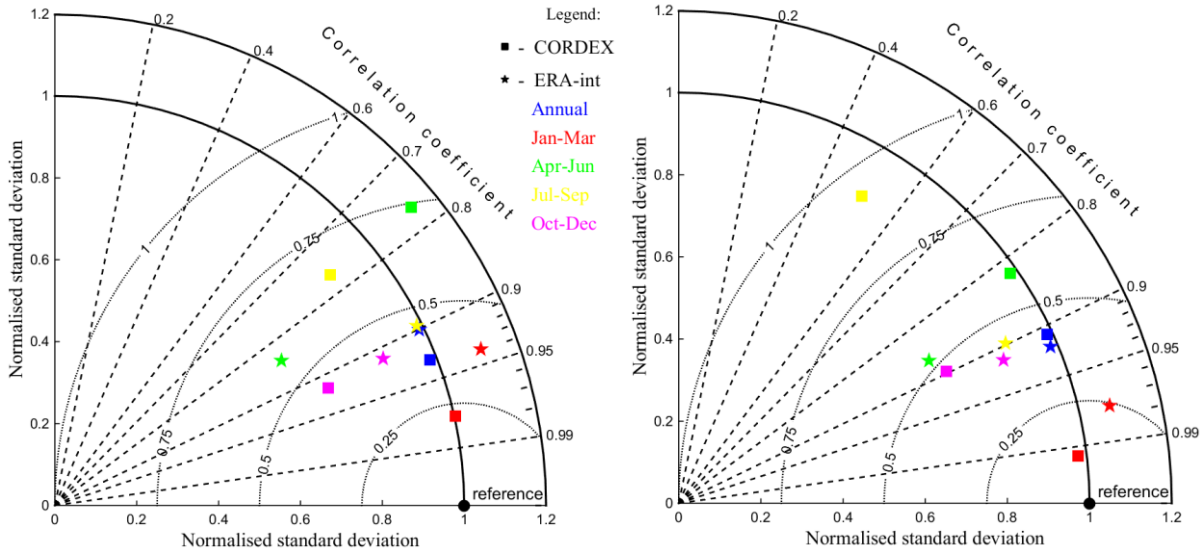

Figure 13. Taylor diagram of the sea surface temperature sensitivity to the atmospheric forcing (squares "■" – CORDEX; asterisks "★" – ERA-int) and underwater attenuation method. On the left the Taylor diagram for $A = 0.7$ on the right – for $A = 0.65$.

2.3.2 Validation

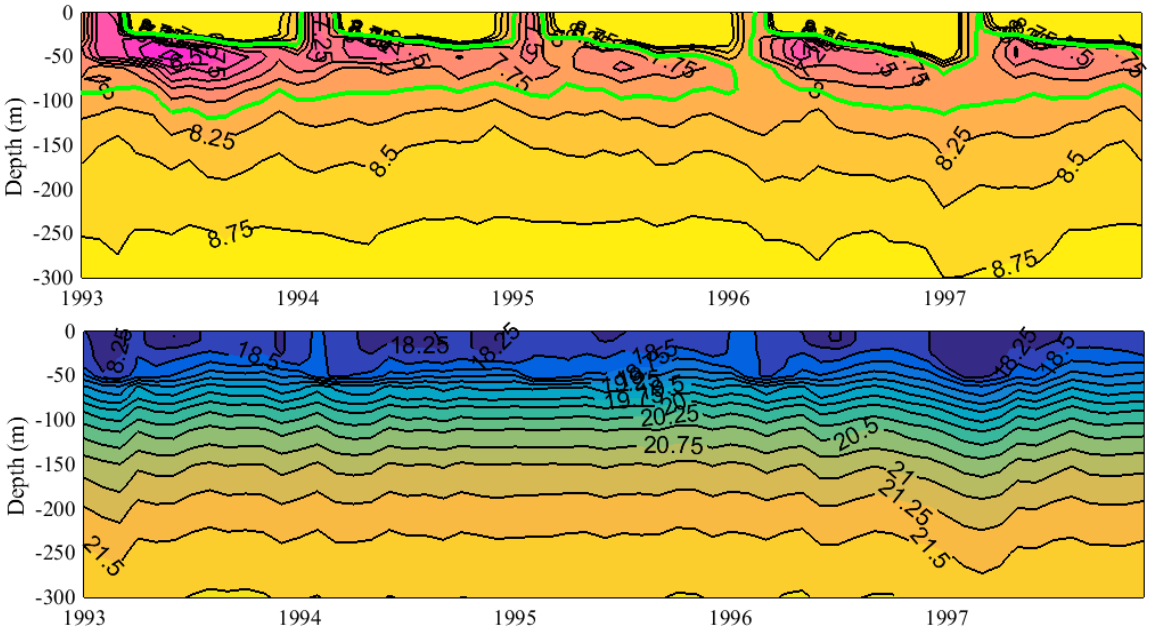

Figure 14. Monthly mean contours of temperature (°C) (upper panel) and salinity (lower panel) from the surface to 300 m depth at b2 – data driven model results from MHI.

Basically, a few hydrographic surveys per year have been conducted in the last 2-3 decades with irregular coverage both in space and time. The first high-quality conductivity/temperature-depth (CTD) data were collected in 1988 (Murray et al., 1991) and used to describe the hydrography and circulation of the whole water column. New hydrographic (temperature, salinity and density) and oxygen/hydrogen sulphide data were collected during two R/V Knorr research cruises to the western part of the Black Sea in a few weeks in 2001 and 2003 (http://www.ocean.washington.edu/cruises/). At

the same time new data was also collected at the north east coast of the Black Sea near Gelendzhik, Russia by researchers from the Southern Branch of the P.P. Shirshov Institute of Oceanology (SBSIO) (Yakushev et al., 2006). The station locations were well situated to study the continental margin areas in the south west, north-western and north-eastern regions. Many other regions are lacking any data.

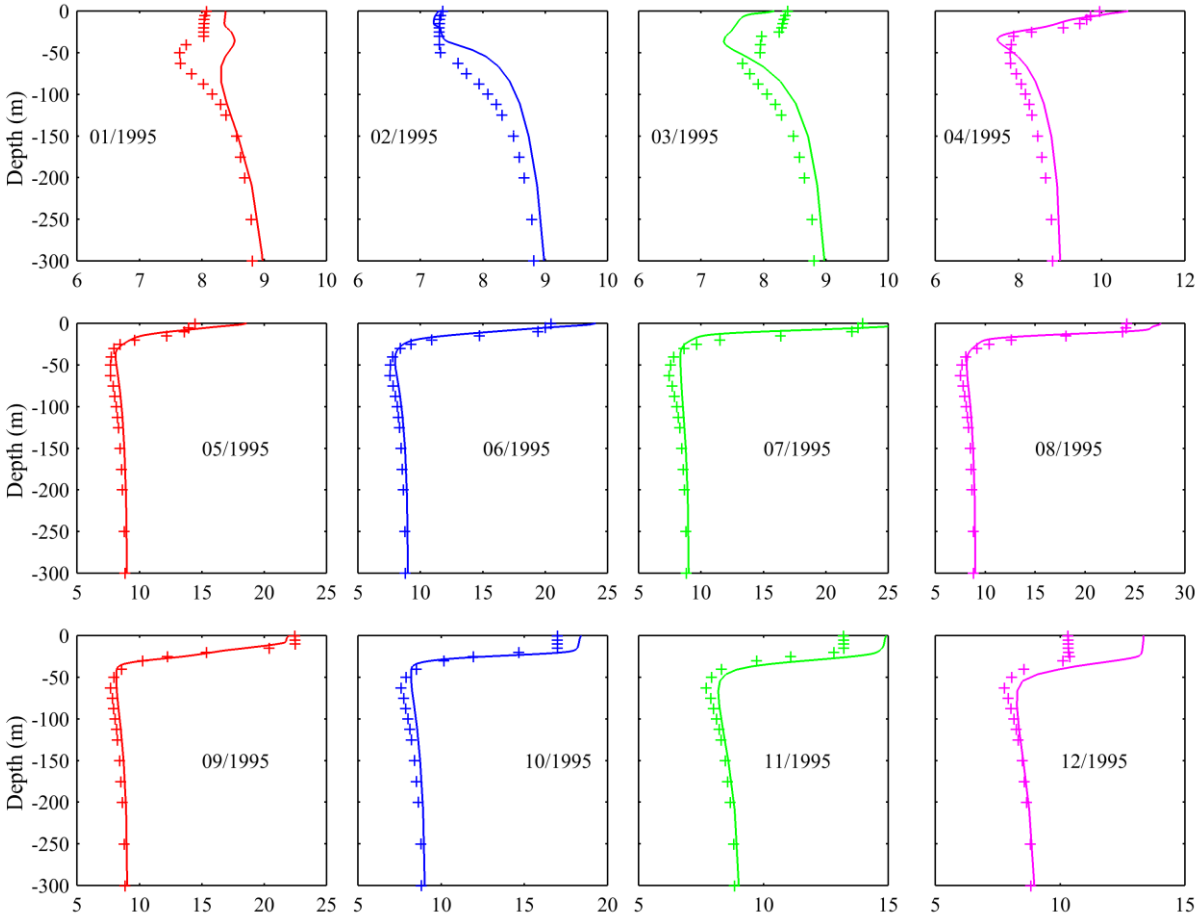

Figure 15. Monthly mean vertical temperature (°C) profiles in 1995 at b2 from the surface to 300 m depth. Our results are denoted with solid lines and MHI results – with symbols.

Monthly mean temperature and salinity profiles of Marine Hydrophysical Institute Ukrainian National Academy of Sciences (MHI, mhi.nas.gov.ua) are used for model validation. These hydrographic profiles for the Black Sea were generated on the basis of satellite remote measurements and models (Black Sea Global Ocean Observing System Project). Data sets from data driven model are available via the SeaDataNet portal (http://www.seadatanet.org/) from 1992 till 2012. For example and comparison, MHI monthly mean contours of temperature (°C) (upper panel) and salinity (lower panel) from the surface to 300 m depth at b2 are depicted in Fig. 14. Seasonal and inter annual variation of temperature/salinity of our model (Fig.12) agrees well with that of MHI model. The main discrepancy was found for the depth and volume of the CIL, as well as our model gives lower values of the surface salinity than MHI's model.

Figs. 14 and 15 represent comparisons of vertical monthly average temperature/salinity profiles in 1995 at b2. We have chosen to present monthly profiles in a particular year and location instead of mean monthly profiles of the whole computation period in order to keep local seasonal and inter-annual variations. The vertical temperature/salinity

distribution in the model agrees well, in both qualitative and quantitative comparisons, to MHI profiles. Moreover, our simulations reproduce closely the annual temperature/salinity cycle as described by MHI data. An interesting effect is found for the salinity in the mixed layer in late summer and fall, namely, there is a layer with lower salinity than that at the surface might be due to the intrusion of fresh and cold water into the open sea upper layers (Fig. 16).

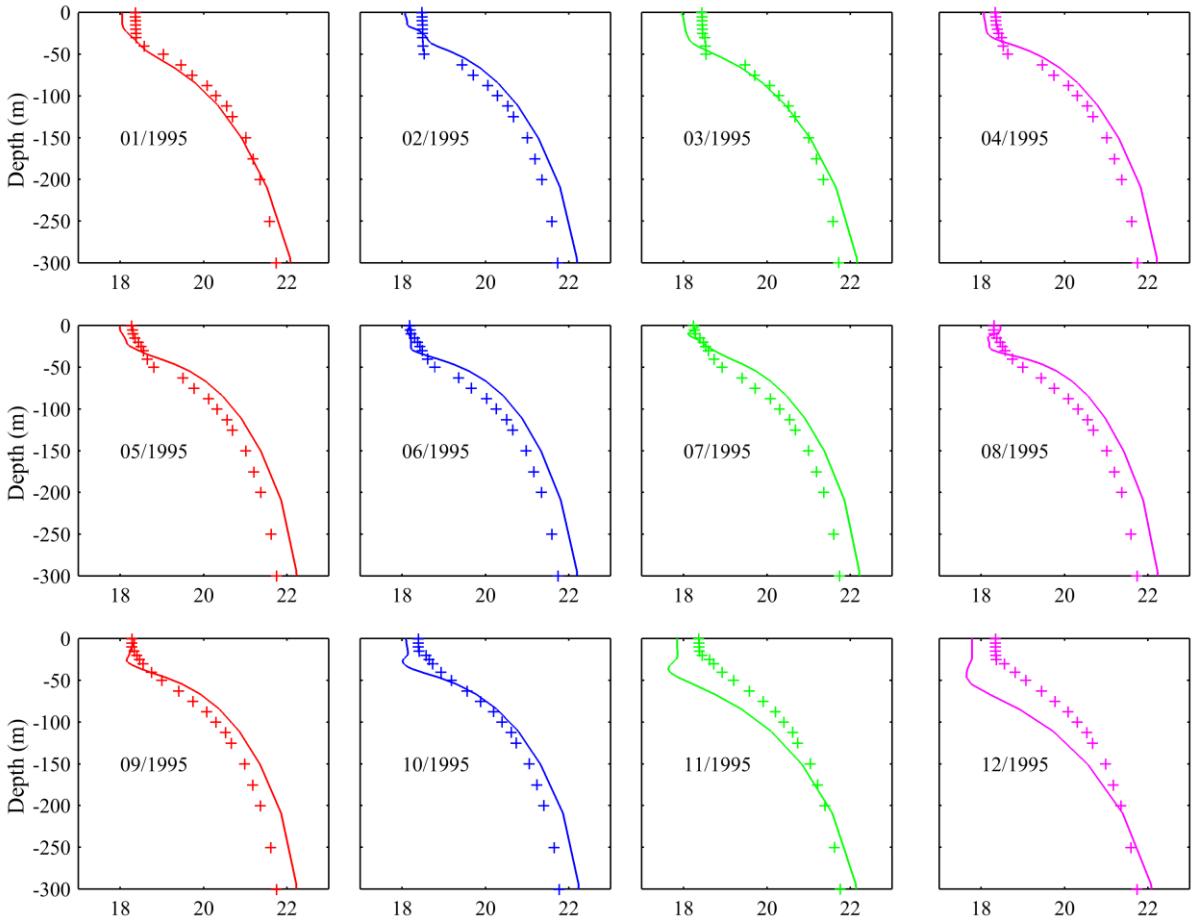

Figure 16. Monthly mean vertical salinity profiles in 1995 at b2 from the surface to 300 m depth. Our results are denoted with solid lines and MHI results – with symbols.

All results presented in this and subsequent paragraphs are calculated using CORDEX and GRDC forcing when is not specifically mentioned the forcing.
Histograms and RMSE are shown in Fig. 17 in order to assess the differences between simulated herein SST and SST of MHI and Pathfinder. Histograms of SST in each month of 1995 are shown as an example of a year in which annual mean SST does not differ significantly from the 20 year mean value. All three sources give very similar distribution of winter temperature (December – March). Both our and MHI's SST values differ significantly from Pathfinder data for April and May with the highest RSMEs. It might be essential to assess the quality of the satellite data. Now, we can conclude that our model calculates SST in accordance with available data, though it gives higher SST in spring and summer. Figures 12, 14-17 complete the model validation process determining that simulations of our hydrodynamic model correctly reflect the Black Sea's hydrodynamics.

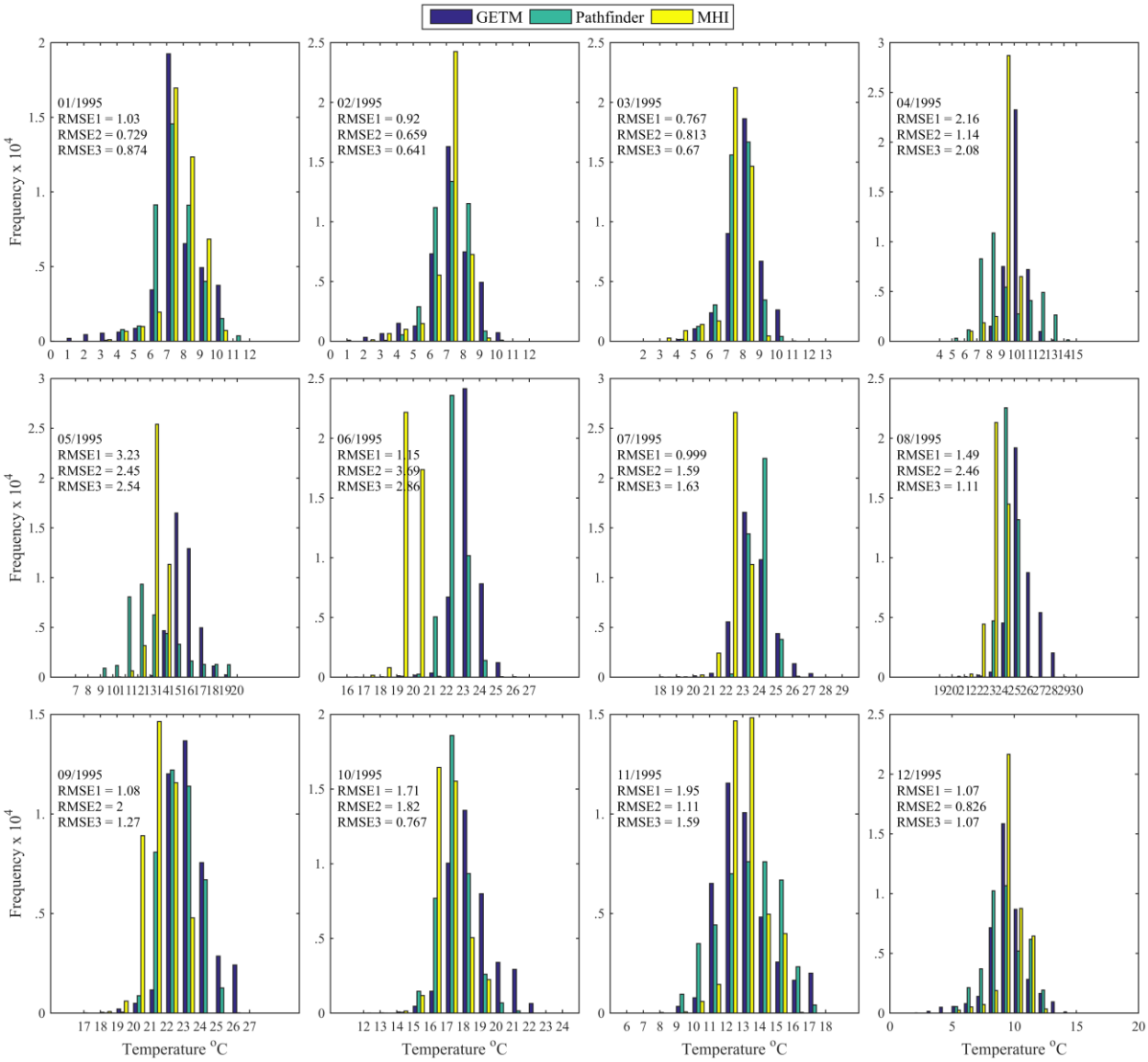

Figure 17. Histograms of the sea surface temperature (°C) in 1995. The base run started in 1990. Green – results of present model (GETM), blue – climatological Pathfinder and yellow – MHI data. RMSE1 (°C) is the root mean squared error between GETM and Pathfinder, RMSE2 (°C) – between GETM and MHI and RMSE3 (°C) – between MHI and Pathfinder.

3. Coupled model

The resultant flow fields from the hydrodynamic model are then used to calculate the evolution of the of the low trophic level components of the food chain in the Black Sea ecosystem. Black Sea's ecosystem model is linked first with the GETM/GOTM hydrodynamic models via the Framework for Aquatic Biogeochemical Models (FABM, Bruggeman and Bolding 2014). FABM is an interface between biogeochemical models and physical models developed to run with GETM/GOTM among many other hydrodynamic models for several computing platforms.

3.1 Ecosystem model

To describe the low trophic level pelagic ecosystem model of the Black Sea, a nitrate-based biogeochemical model has been implemented following the existing literature (e.g., Oguz et al., 2000, 2001, 2006, 2008, 2014). This model provides an optimally

complex system of food web interactions and biogeochemical cycles comprising oxic-, suboxic- and anoxic waters of the Black Sea. It represents the classical omnivorous food-web with 7 state variables. These include two phytoplankton size groups (small and large), four zooplankton groups including micro- and mesozooplankton, non-edible dinoflagellate species as *Noctiluca,* and the gelatinous zooplankton species *Mnemiopsis.* The nitrogen is represented by two inorganic nutrients (nitrate and ammonium) and included in the particulate organic material (detritus). Additional state variables are dissolved oxygen and hydrogen sulphide. This system offers an optimal complexity with medium complex trophic interactions as shown in Figure 6. The full set of equations describing this ecosystem is provided in Oguz et al. 2014. Hereinafter this model will be referred to as BSSM. BSSM has been implemented into the FABM and is available for the scientific community.

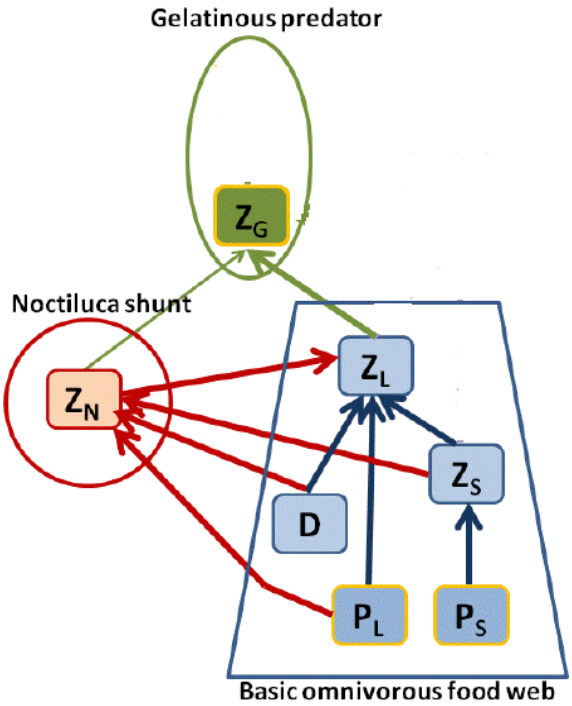

Figure 18. Schematic representation of the BSSM structure that includes the basic omnivorous food web and its interactions with the gelatinous carnivore predator and *Noctiluca shunt*.

3.1.1 BSSM setup

The initial conditions of BSSM variables are chosen from Knorr 2001/2003 experimental data (Cannaby et al, 2015; Tugrul et al., 2014; Stanev et al., 2014). They reproduce mainly the observed characteristics near north-western and south-western shelf of the Black Sea ecosystem. Nitrate concentration is set to 0.33 mmol N/m^3 within the upper 10 m, then it increases to 3.7 mmol N/m^3 between 15m and 35 m depths and decreases to zero at 100 m. Ammonium is set to 0.03 mmol N/m^3 within the upper 90 m, then it increases linearly to 70 mmol N/m^3 between 90 m and 450 m depths and remains a constant till the sea bottom. Hydrogen sulphide is zero in the upper 90 m, then it increases linearly to 860 mmol HS/m^3 at the sea bottom. Dissolved oxygen decreases linearly from 360 mmol O_2/m^3 to 0 in the upper 70 m and is set to zero further below. All the other BSSM's state variables are set to small and vertically uniform values over the entire water column because their equilibrium structures do not depend on the initial conditions and are emergent properties of the model dynamics.

The coupled runs begin in June 1990 to allow adjustment of the hydrodynamic model. Climatological riverine load of nutrients (http://www.ifremer.fr/medar/) is incorporated.

3.1.2 BSSM sensitivity

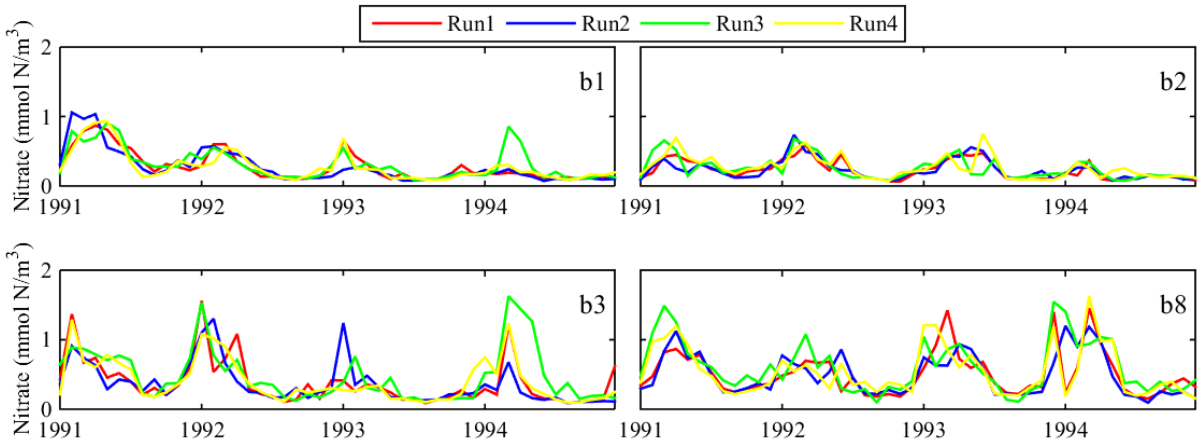

Figure 19. Maximum nitrate concentration (mmol N/m^3) at four particular locations, namely at b1, b2, b3 and b8 (see Fig. 1). Time series of monthly mean values in 4 case studies are presented with different colours.

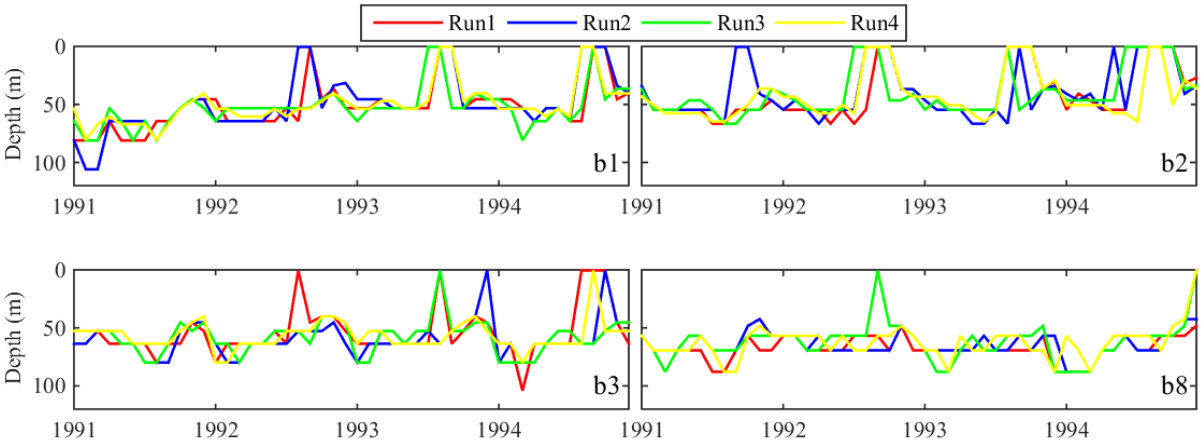

Figure 20. Monthly mean depth (m), at which maximum nitrate concentration occurs (shown in Fig. 19).

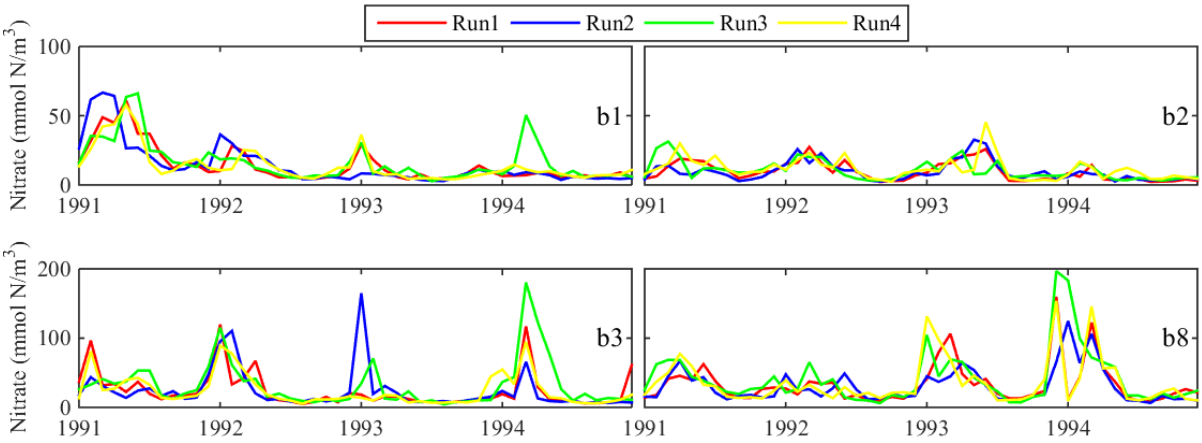

Figure 21. The same as in Fig. 19 but for depth integrated nitrate.

In the following BSSM sensitivity to riverine nutrient loads will be illustrated. Four case studies with different nutrient load are run: Run1 – without nutrient load; Run2 – Danube River nitrate load only; Run3 – climatological nitrate load of all nine rivers considered in the model; Run4 – twice as high in Run3.

Time series of maximum and depth integrated nitrate at b1, b2, b3 and b8 are plotted in Figs. 19 and 21, respectively. Nitrate distribution undergoes clear seasonal cycle in all runs. Regional changes in maximum nitrate are dominated by the circulation/vertical mixing intensity. Locations b1 and b2 are exposed to upwelling in the centre of cyclonic gyres and they are far from the Rim current, so seasonal variation in nitrate is less pronounced. Moreover, the depth integrated nitrate is approximately a half of that in b3 and b8. Due to heavy nitrate load of the Danube, Dniepr and Dniestr rivers, simulated maximum nitrate concentrations on the north-western shelf were very high (~36 mmol N/m^3 for Run4), however the depth integrated concentrations are similar to that in b3 due to the thicker nitrate rich layers. Obviously, the periphery of the Black Sea's interior, along the Rim jet contains much higher nitrate concentrations than in the central basin. It is worth to note that calculate herein nitrate in b3 and b8 is about a half of measured values (Cannaby et al, 2015; Tugrul et al., 2014; Stanev et al., 2014), thus further calibration of BSSM model or boundary conditions is necessary to be done. The role of nitrate load is not clear because there are picks of both maximum and depth integrated nitrate that are higher in cases with lower loads. The depth where a maximum nitrate arises (~50 m) is actually the upper halocline (see Fig. 20) which in a perfect accordance with experimental evidence.

3.2 Simulations and verification

Time series of main model variables at locations b1 and b3, resulting from the Run4 are shown in Figs. 22 and 23. The near surface layer of about 50 m thickness, so called mixed layer (ML), is the layer of active biological processes (uptake, grazing, mortality, etc.). Typically, in it the concentration of oxygen is high (more than 200 mmol O_2/m^3), nitrate and organic matter (detritus) concentrations vary seasonally. In the Black Sea's interior this layer is scarce in nutrients for most of the year except for vertical winter mixing and occasional intrusion from coastal regions. Below ML nitrate concentration rises and supports summer subsurface production of large phytoplankton. In winter, nitrate in the ML is renewed primarily from the upper part of the halocline through vertical diffusion, buoyancy induced mixing and upwelling, and depleted by biological utilisation. The large part of particulate organic matter (see detritus contours in Figs. 22 and 23) is remineralised inside ML and the subsequent 10 – 20 m part of oxygenated zone. Only small part of detritus particles sink to deeper anoxic part of the sea - about 100 m depth (Fig. 22) and to 150 m depth (Fig. 23). Karl and Knauer, 1991 reported that this depth is shallower in the sea interior (about 100 m) and about 200 m in the onshore, anticyclonically dominated zone and the same conclusion is maintained by our simulations. Note that results presented in Fig. 23 are taken at b3 – a location, where the nitrate is higher than at b1 and subsequently the plankton production is higher. For example, vertical distributions of total phytoplankton and total zooplankton in 1992 very well agree with model results of Dorofeyev et al., 2012. Seasonal and inter-annual evolution of presented state variables in b1 (Fig. 22) and b2 (Fig. 23) are similar to each other. Nitrate is nearly depleted from the ML in summer/fall. Oxygen anoxic zone begins approximately from the bottom of the CIL, where the onset of ammonium and hydrogen sulphide starts. Small phytoplankton exhibits substantial annual grow in the ML above the CIL with a decline in summer. Large phytoplankton has blooms in summer in the zone below the ML and smaller blooms during winter in ML. Zooplanktons bloom in winter/spring. Noctiluca blooms in spring and in warmer years there is second bloom in summer. Annual phyto- and zooplankton structure corresponds to available data and

model simulations summarised in Oguz et al., 2004. The model reproduces correctly the blooming periods. Consequently, the concentration of detritus increases in winter/spring in the ML and in late summer/fall displays maxima in the CIL. The last result is supported by Yakushev et al., 2007, who reported for the presence of turbidity layer in the vicinity of hydrogen sulphide onset.

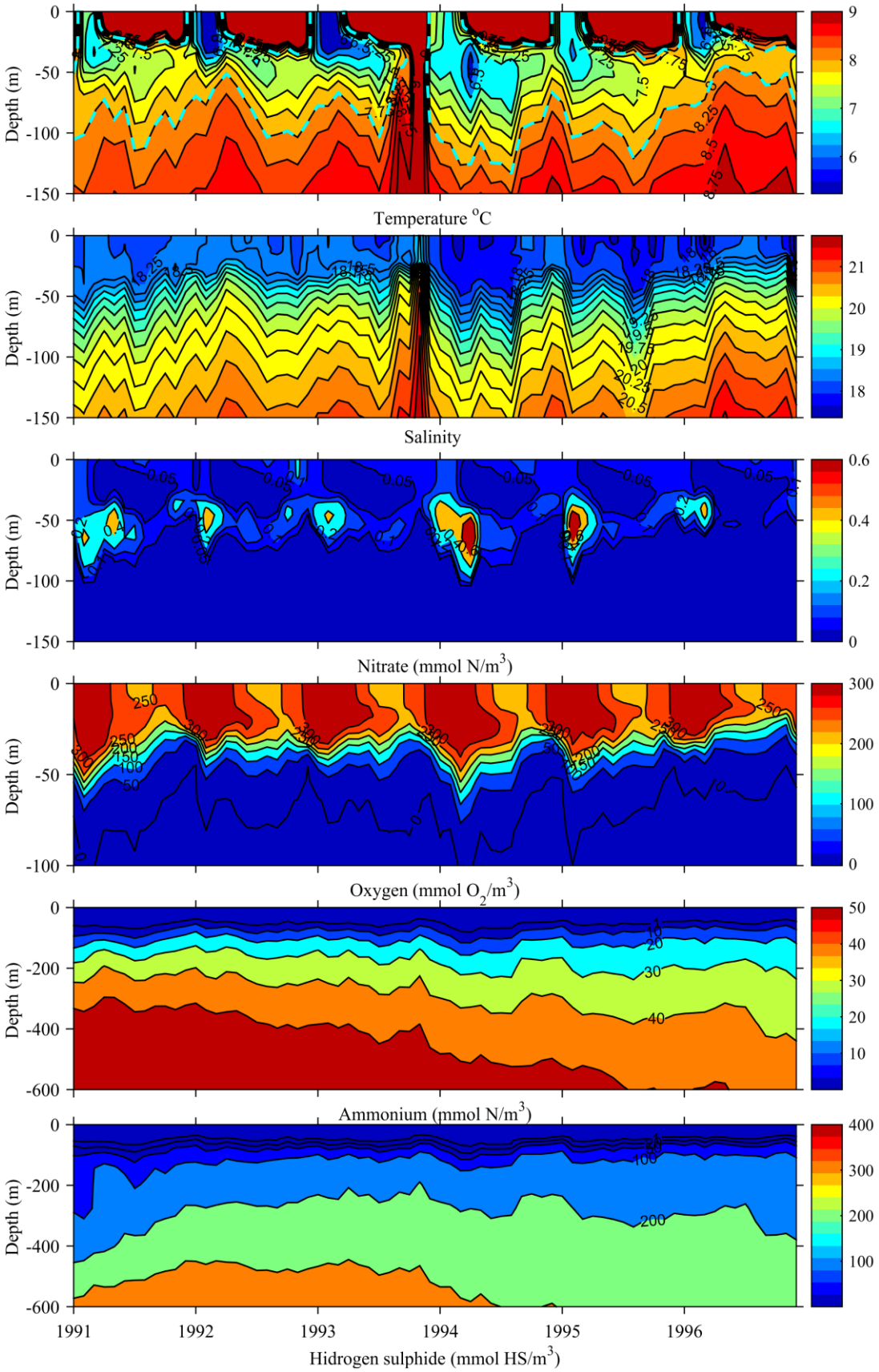

(Continue on the next page)

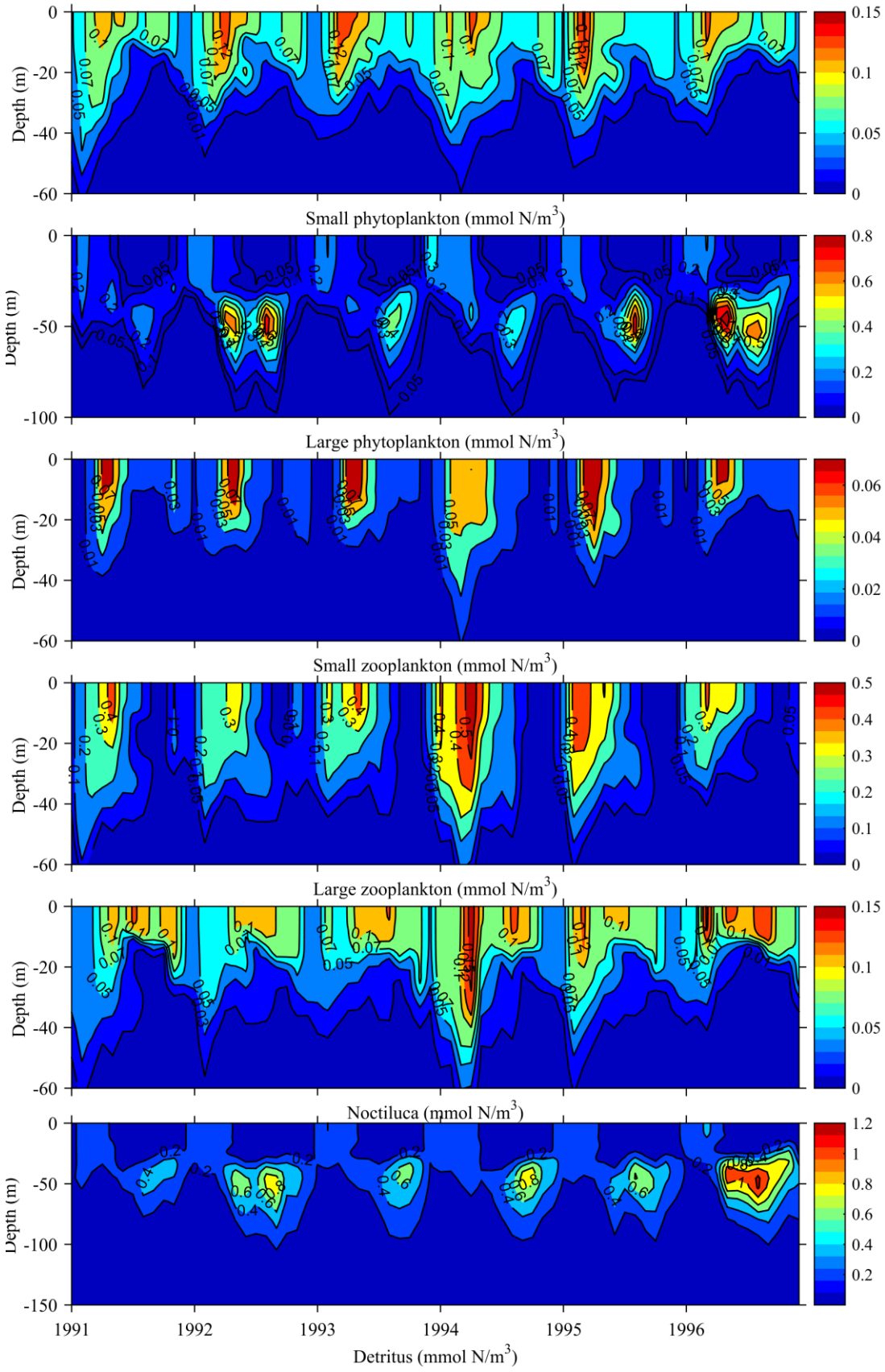

Figure 22. Evolution of temperature (°C), salinity, nitrate (mmol N/m^3), oxygen (mmol O_2/m^3), ammonium (mmol N/m^3), hydrogen sulphide (mmol HS/m^3) (upper panel); small phytoplankton, large phytoplankton, small zooplankton, large zooplankton,

Noctiluca and detritus in mmol N/m^3 (lower panel) from the surface to 150 m depth at b1.

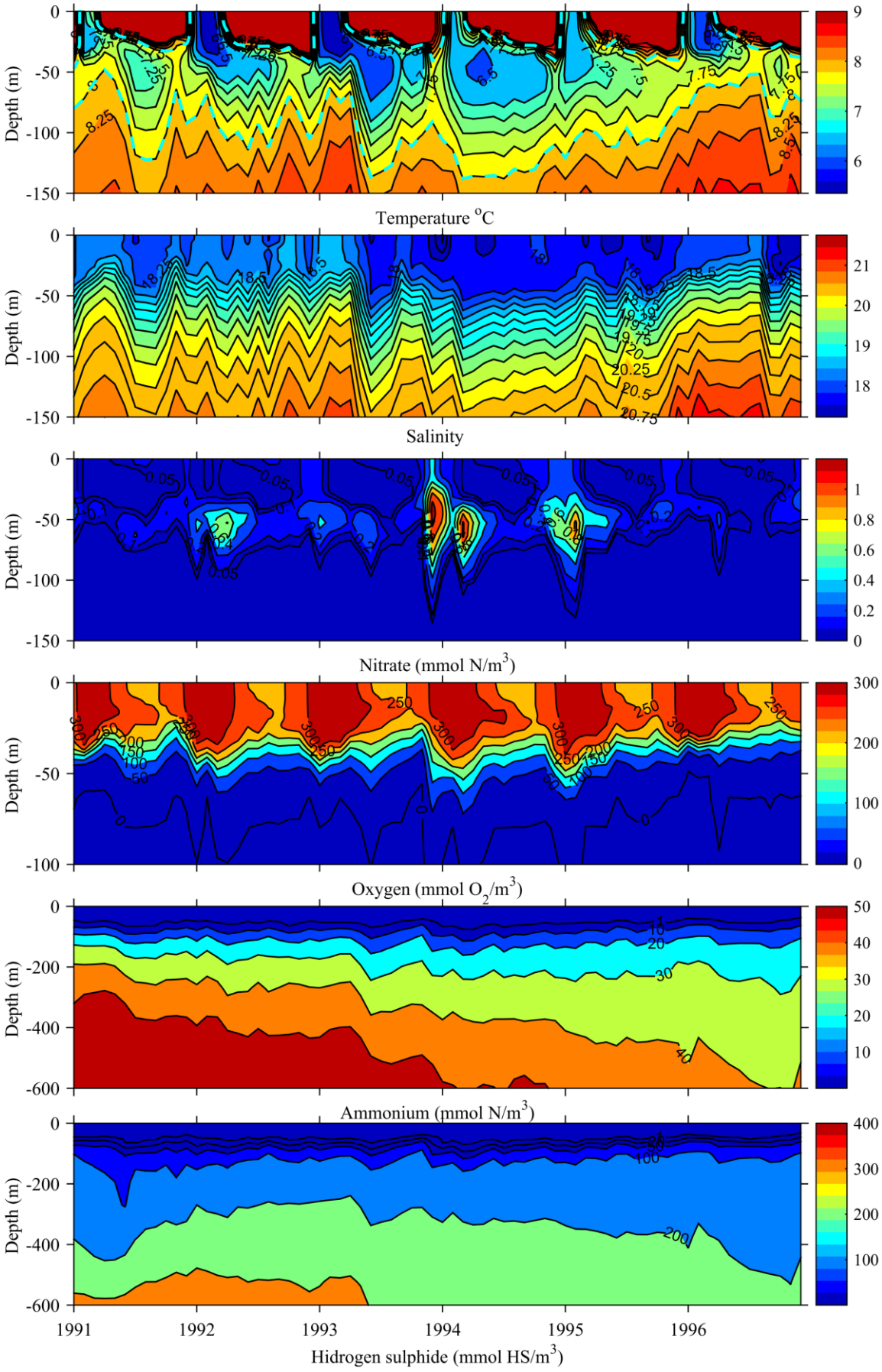

(Continue on the next page)

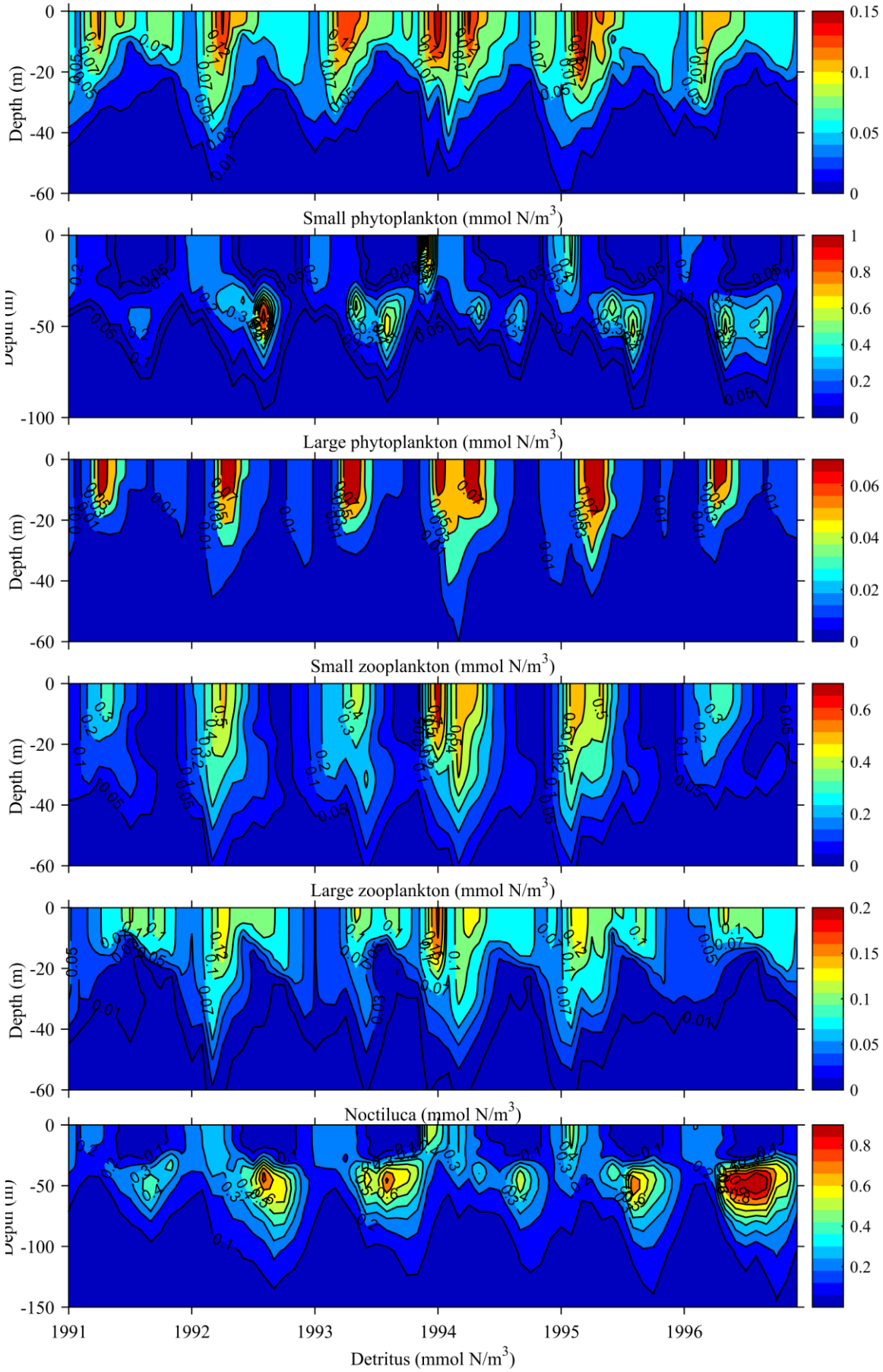

Figure 23. The same as in Fig. 22 but at b3.

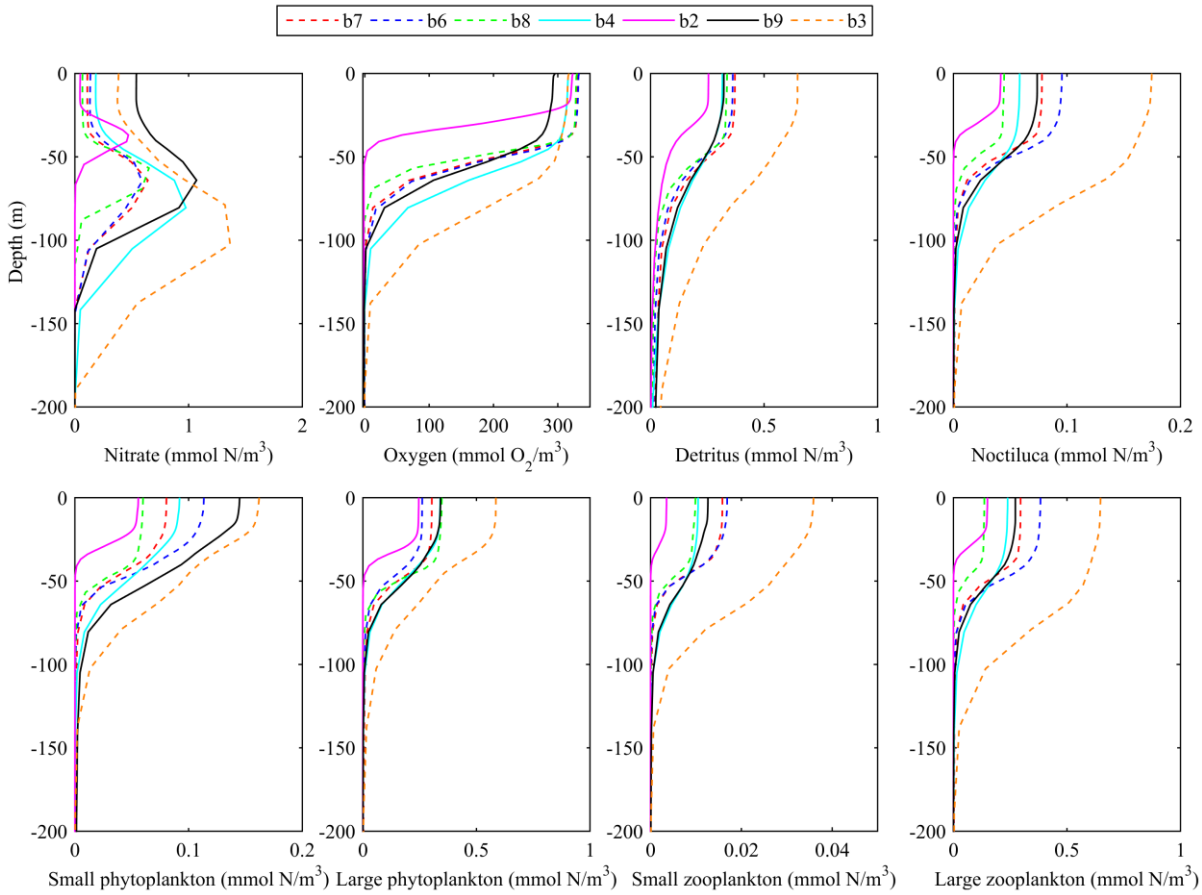

Figure 24. Vertical profiles of nitrate (mmol N/m^3), oxygen (mmol O_2/m^3), detritus, *Noctiluca*, small phytoplankton, large phytoplankton, small zooplankton and large zooplankton (mmol N/m^3) from the surface to 200 m depth in February 1992 at different location in the Black Sea (see the legend).

Seasonal changes in the Black Sea ecosystem in certain locations are illustrated in Figs. 24 and 25, where mean vertical profiles of ecosystem components are plotted in February (Fig. 24) and in July (Fig. 25). The overall impression is that the vertical variation of ecosystem components throughout the basin is more pronounced in winter (Fig. 20) when mixing is more intensive. The formation of a seasonal thermocline in the surface layer and the presence of a strong halocline formed just below the CIL limits vertical exchange with deep waters and leads to the formation of nitracline and oxic/anoxic transition layer (oxycline) in the permanent halocline. The depth distribution of nitrate displays a distinct vertical structure over the basin. It reaches a maximum (Fig. 20) in the CIL, which is deepening from the central basin to the Rim current and anticyclonic eddies in the coastal zone. Note, that the depth distribution of nitrate demonstrates highest values at 42°N and 32°E (dashed yellow line) in the Rim current area. Additionally, winter oxygen penetration is the deepest in this location. The oxygen deficient (< 10 mmol O_2/m^3), sulphide free layer with a thickness of 10 - 50 m, is consistent with the lower nitracline zone, called as suboxic layer (Murray et al., 1991). Other variables have maxima in the upper ML and decrease to zero in the CIL in February (Fig. 24). In July (Fig. 25) the depth profiles of state variables obey similar distributions in all presented locations. The formation of seasonal thermocline since March restricts the penetration of oxygen and biomass production is concentrated in the ML resulting in nitrate depletion. Large phytoplankton and zooplankton, and *Noctiluca*, however sink and grow successfully till 60 – 80 m depth. Depending on the strength of

summer, small phytoplankton productivity, the near surface oxygen concentrations are lower than the mean ML concentrations. Obviously, large phytoplankton have found better growth conditions below thermocline and above halocline where nitrate concentrations are higher. In general, our simulations show similar behaviour as in situ measured data (see Tugrul et al. 2014) where the maxima in the vertical nitrate profiles are higher.

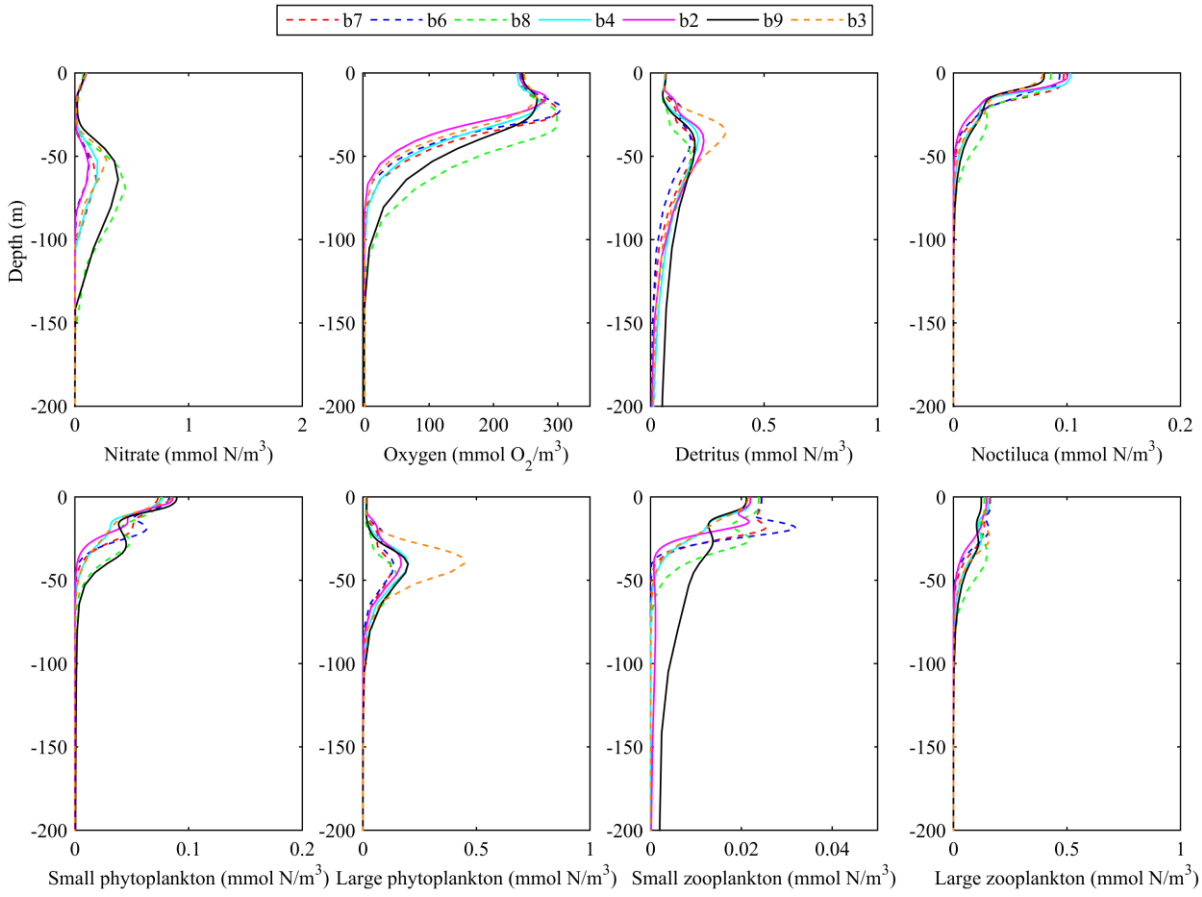

Figure 25. The same as in Fig.24 but in July 1992.

4. Conclusions

The evolution of the Black Sea ecosystem has been calculated using 3D high resolution (2 min by 2 min grid) hydrodynamic (GETM/GOTM) and biogeochemical model (BSSM). First, several river discharge data sets covering the Black Sea have been examined and GRDC has been chosen to define the river loads in our model. Next, four different historical climatological reanalysis were assessed by comparing their precipitation/evaporation data. The ERA-int and downscaled CORDEX erain forcing were the preferred ones. On the base of GRDC runoff and ERA-int/CORDEX precipitation/evaporation the freshwater input was evaluated. Based on the calculated freshwater input, in situ data and climatological mean values of the inflow/outflow from the Bosphorus Strait, the inflow/outflow profiles have been updated annually in order to keep the sum of inflow and outflow equal to freshwater input. High resolution (2 min by 2 min) bathymetry grid is produced from ETOPO1 global bathymetric grid with horizontal resolution of 1 min. Linear programming procedure was applied to smooth slightly the bathymetry. The model is initialised by means of temperature and salinity 3D fields coming from the project MEDAR/MEDATLAS II. An accurate method for evaluation of water optical characteristics by means of an optical depth estimated from the satellite data has been involved. Finally, the performance of the model in simulating the Black Sea's physical properties at seasonal and inter-annual scales have been assessed by comparing model outputs with satellite SST, occasional in situ measurements and independent calculations of temperature and salinity fields. The correlation between modelled herein SST and that from other sources is good, as well as vertical temperature/salinity profiles match well MHI's data. Upper and deep water circulation, thermohaline structure, temporal and space variability of the Rim current and Cold Intermediate Layer were simulated correctly by the model.

BSSM is considered as a biogeochemical model of the Black Sea ecosystem. It is linked with the hydrodynamic model by FABM. Numerical calculations with the coupled model provides a useful tool supporting advanced studies of the spatial and temporal variation of the ecosystem. Due to the lack of regular measurements, model results are validated qualitatively against sporadic measurements and independent calculations. Our simulations show early spring bloom of small phytoplankton and a subsequent increase in zooplankton growth that is in accordance with modelling studies (Oguz et al., 1999 and 2001) and it is a specific characteristic of the annual plankton structure of the Black Sea ecosystem, which has been seen in every dataset irrespective of the type top-down grazing control by top-predators (Sorokin, 2002).

Nevertheless, that the north-western shelf area is rich of nutrients (mainly due to Danube runoff) this contribution is not the main source of nutrients in the deep sea area. Nitrate load from rivers is mainly spread and circulating along the Rim current. It is found that vertical flux of nutrients from pycnocline in winter is a key factor for phytoplankton growth in sea interior and supports new production. We can conclude that the physical factors, like winter vertical mixing, CIL's volume and temperature, Rim jet velocity, SST and photosynthetically active radiation are the key factors that control the bio-chemical processes in the Black Sea.

References

Beşiktepe Ş, Sur HI, Özsoy E, Latif MA, Oğuz T, Ünlüata Ü: The circulation and hydrography of the Marmara Sea. Prog Oceanog 34:285–334, 1994

Beşiktepe Ş.: Coupled physical and biochemical data driven simulations of Black Sea in spring-summer: real-time forecast and data assimilation. Elsevier Oceanography Series, 69:203–210, 2003

Bruggeman, J. and Bolding, K.: A general framework for aquatic biogeochemical models.

Environmental Modelling and Software, 61, 249–265, 2014.

Dorofeyev, V.,T.,Oguz, L. I. Sukhikh, V. V. Knysh, A. I. Kubryakov and G. K. Korotaev: Modeling long-term changes of the Black Sea ecosystem characteristics,Ocean Sci. Discuss., 9, 2039–2080, 2012

Josey, S. A., R. W. Pascal, P. K. Taylor, and M. J. Yelland : A new formula for determining the atmospheric longwave flux at ocean surface at mid-high latitudes, J. Geophys. Res., 108(C4), 3108, 2003, doi:10.1029/ 2002JC001418.

Kara, A.B., Wallcraft, A.J. and Hurlburt, H.E.: How does solar attenuation depth affect the ocean mixed layer? Water turbidity and atmospheric forcing impacts on the simulation of seasonal mixed layer variability in the turbid Black Sea. J. Climate, 18:389–409, 2005.

Karl, D.M., and G.A. Knauer. Microbial production and particle flux in the upper 350 m of the Black Sea. Deep Sea Res., 38, Supp. 2A, S655-S661, 1991

Maderich, V., Konstantinov, S.: Seasonal dynamics of the system sea-strait: Black Sea-Bosphorus case study, Estuarine, Coastal and Shelf Sciences, 55, 183-196, 2002.

Murray, J. W., Z. Top, and E. Ozsoy. Hydrographic properties and ventilation of the Black Sea. Deep-Sea Res., 38, Suppl.2A, S663–690 , 1991

Oguz,T. and L. Rozman. Characteristics of the Mediterranean underflow in the southwestern Black Sea continental shelf/slope region. Oceanology Acta, 14(5), 433.444. , 1991

Oguz, T., H. Ducklow, P. Malanotte-Rizzoli, J.W. Murray, V.I. Vedernikov, and U. Unluata. A physical-biochemical model of plankton productivity and nitrogen cycling in the Black Sea. Deep-Sea Res. I. 46, 597–636. , 1999

Oguz, T., Ducklow, H.W., and Malanotte-Rizzoli, P.: Modeling distinct vertical biogeochemical structure of the Black Sea: dynamical coupling of the oxic, suboxic and anoxic layers, Global Biogeochem. Cy., 14, 1331–1352, 2000.

Oguz, T., H. W. Ducklow, J. E. Purcell, and P. Malanotte-Rizzoli. Modeling the response of topdown control exerted by gelatinous carnivores on the Black Sea pelagic food web. J. Geophys. Res., 106, 4543–4564. , 2001

Oguz, T., Tugrul, S., Kideys, A.E., Ediger, V.and Kubilay, N.: Physical and biogeochemical characteristics of the Black Sea (28,S), in: The Sea, vol. 14, edited by: Robinson, A. R. and Brink, K. H., Harvard University Press, chap. 33, 1331–1369, 2004.

Oguz T, Merico: A Factors controlling the summer *Emiliania huxleyi* bloom in the Black Sea: a modelling study. J Mar Syst 59:173–188, 2006.

Oguz, T., B. Salihoglu, and B. Fach, "A coupled plankton–anchovy population dynamics model assessing nonlinear controls of anchovy and gelatinous biomass in the Black Sea," Mar. Ecol. Prog. Ser. **369**, 229–256 ,2008.

Oguz, T., Stips, A., Macias, D., Garcia-Gorriz, E. and Coughlan, C.: Development of the Black Sea specific ecosystem model (BSSM), Technical report, EUR27003EN, European Commission, Ispra, 2014.

Ovchinnikov, I.M., Popov, Yu.I. : Formation of a cold intermediate layer in the Black Sea. Oceanology 27, 739–746. , 1987

Peneva, E. L. and Stips, A. K.: Numerical simulations of Black Sea and adjoined Azov Sea, forced with climatological and meteorological reanalysis data, Technical report, EUR21504EN, European Commission, Ispra, 2005.

Sorokin, Y.I., 2002. The Black Sea ecology and oceanography. Backhuys Publishers, Leiden, 875 pp.

Stanev, E., He, Y., Staneva, J. and Yakushev, E.:Mixing in the Black Sea detected from the temporal and spatial variability of oxygen and sulfide – Argo float observations and numerical modelling, Biogeosciences, 11, 5707–5732, 2014

Stips A, Bolding K, Pohlmann T, Burchard H: Simulating the temporal and spatial dynamics of the North Sea using the new model GETM (General Estuarine Transport Model). Ocean Dynamics, 54, 266-283, 2004

Tugrul, S., Beşiktepe Ş, and Salihoglu. I.: Nutrient exchange fluxes between the Aegean and Black Seas through the Marmara SeaMediterranean Marine Science, Vol. 3/1, 33-42, 2002

Zatsepin, A. G., A. I. Ginzburg, A. G. Kostianoy, V. V. Kremenetskiy, V. G. Krivosheya, S. V. Stanichny, and P.-M. Poulain, Observations of Black Sea mesoscale eddies and associated horizontal mixing, J. Geophys. Res., 108(C8), 3246, doi:10.1029/2002JC001390, 2003.

Ünlüata, Ü., Oguz, T., Latif, M. A., and Özsoy, E.: On the physical oceanography of the Turkish straits, in: NATO ASI, edited by: Pratt, L. J., 25–60, 1990

Yakushev, E. V., Pollehne, F., Jost, G., Kuznetsov, I., Schneider, B., and Umlauf, L.: Analysis of the water column oxic/anoxic interface in the Black and Baltic seas with a numerical model, Mar. Chem., 107, 388–410, 2007.

List of abbreviations and definitions

b1 - 43°N and 32°E
b2 - 43°N and 38°E
b3 - 42°N and 31°E
b4 - 42°N and 39°E
b5 - 43°N and 34°E
b6 - 43°N and 31°E
b7 - 42°N and 30°E
b8 - 44°N and 32°E
b9 – 44.5°N and 37°E
BSSM: Black Sea Specific Ecosystem Model
CIL: Cold Intermediate Layer
CORDEX erain: atmospheric dataset produced by CCLM with ERA-interim reanalysis
CTD: conductivity/temperature-depth
ECMWF: European Center for Medium Range Weather Forecast
ERA40: ECMWF ERA 40 reanalysis
ERA-int: ECMWF ERA-interim reanalysis
ETOPO1: Earth topography database
EU: European Union
FABM: Framework for Aquatic Biogeochemical Models
GRDC: Global River Data Center database
GETM: General Estuarine Ocean Model
JRC: Joint Research Centre
MC: Marie Curie
ML: Mixed layer
MEDAR/MEDATLAS: Mediterranean Data Archaeology and Rescue database
MHI: Marine Hydrophysical Institute Ukrainian National Academy of Sciences
MSFD: Marine Strategy Framework Directive
N: Nitrate
NCEP: National Centres for Environmental Prediction
NRL: Naval Research Laboratory
RMSE: root mean squared error
RivDIS: Global River Discharge Database
SIMSEA: Scenario simulations of the changing Black Sea ecosystem
SeaWiFS: Sea viewing Wide Field of view Sensor
HS: Hydrogen sulphide
SST: Sea surface temperature
topo2: 2-minute gridded Black Sea relief
topo3: 3-minute gridded Black Sea relief
UCAR: University Corporation for Atmospheric Research
WOA05: World Ocean Atlas 2005 database

List of figures

Figure 19. Maximum nitrate concentration (mmol N/m^3) at four particular locations, namely at b1, b2, b3 and b8 (see Fig. 1). Time series of monthly mean values in 4 case studies are presented with different colours.

Figure 20. Monthly mean depth (m), at which maximum nitrate concentration occurs (shown in Fig. 19).

Figure 21. The same as in Fig. 19 but for depth integrated nitrate.

Figure 22. Evolution of temperature (°C), salinity, nitrate (mmol N/m^3), oxygen (mmol O_2/m^3), ammonium (mmol N/m^3), hydrogen sulphide (mmol HS/m^3) (upper panel); small phytoplankton, large phytoplankton, small zooplankton, large zooplankton, *Noctiluca* and detritus in mmol N/m^3 (lower panel) from the surface to 150 m depth at b1.

Figure 23. The same as in Fig. 22 but at b3.

Figure 24. Vertical profiles of nitrate (mmol N/m^3), oxygen (mmol O_2/m^3), detritus, *Noctiluca*, small phytoplankton, large phytoplankton, small zooplankton and large zooplankton (mmol N/m^3) from the surface to 200 m depth in February 1992 at different location in the Black Sea (see the legend).

Figure 25. The same as in Fig.24 but in July 1992.

List of tables

How to obtain EU publications

Our publications are available from EU Bookshop (http://bookshop.europa.eu),
where you can place an order with the sales agent of your choice.

The Publications Office has a worldwide network of sales agents.
You can obtain their contact details by sending a fax to (352) 29 29-42758.

LB-NA-27786-EN-N

JRC Mission

As the Commission's in-house science service, the Joint Research Centre's mission is to provide EU policies with independent, evidence-based scientific and technical support throughout the whole policy cycle.

Working in close cooperation with policy Directorates-General, the JRC addresses key societal challenges while stimulating innovation through developing new methods, tools and standards, and sharing its know-how with the Member States, the scientific community and international partners.

Serving society
Stimulating innovation
Supporting legislation

doi:10.2788/601495

ISBN 978-92-79-57237-1